Quantifying glacial moraine age, denudation, and soil mixing with cosmogenic nuclide depth profiles

M. Schaller,[1] T. A. Ehlers,[1] J. D. Blum,[1] and M. A. Kallenberg[2]

Received 17 October 2007; revised 13 August 2008; accepted 17 October 2008; published 4 February 2009.

[1] Glacial boulders and soils on moraines are often dated to quantify the timing of glaciations and/or rates of chemical weathering in moraine chronosequences. A common assumption is that moraine crest erosion and soil mixing are unimportant. However, several studies suggest moraine denudation may be substantial. We evaluate the magnitude of moraine denudation and soil mixing in the Pinedale (~21 ka) and Bull Lake (~140 ka) moraines at Fremont Lake (Wyoming, United States) using cosmogenic nuclide depth profiles and a numerical model of moraine erosion and nuclide production and decay. Depth profiles indicate mixing of the surface layer from 40 to 60 cm depth. Age constraints from depth profile dating of cosmogenic nuclides result in ages of 17–24 ka for the Pinedale moraine and 70–127.5 ka for the Bull Lake moraine. These ages are comparable to ages based on the Lal and Chen approach which uses a sample from the mixed layer and the unmixed layer. However, the Lal and Chen approach is difficult to apply in real environments as the mixing depth needs to be determined independently. We find our best fit model based ages for the Bull Lake moraine are younger than independent age constraints from boulder exposure dating due to incomplete mixing. Exposure age constraints from boulders are more straightforward for moraines than ages based on depth profile dating. Finally, we find that moraine crests do significantly erode and are mixed, suggesting that previous weathering and dust accumulation rate studies on moraines provide minimum estimates for these processes.

Citation: Schaller, M., T. A. Ehlers, J. D. Blum, and M. A. Kallenberg (2009), Quantifying glacial moraine age, denudation, and soil mixing with cosmogenic nuclide depth profiles, *J. Geophys. Res.*, *114*, F01012, doi:10.1029/2007JF000921.

1. Introduction

[2] Moraines mark the past extent of glaciers and reveal information about glacial fluctuations due to climatic change. The age of moraine deposition is important for absolute time constraints of these events. Techniques often used to constrain moraine deposition ages include surface exposure age dating of boulders, radiocarbon dating, and U-series disequilibrium. Alternatively, moraine deposition can be dated by measurement of in situ–produced cosmogenic nuclides in soil depth profiles. The utility of cosmogenic nuclides from soil depth profiles to quantify glacial moraine age, denudation, and soil mixing in two moraines of different age in Wyoming (United States) are evaluated. The implications of our results to other study areas are discussed.

[3] Application of cosmogenic nuclides in depth profiles to determine sediment deposition ages, denudation rates, and study soil processes has a long tradition. The technique of exposure age dating has been applied to cobbles from sedimentary deposits [e.g., *Trull et al.*, 1995], along with recognition that the measured nuclide concentrations need to be corrected for inherited nuclides accumulated during sediment production and transport [*Anderson et al.*, 1996]. The inherited nuclide concentration can be determined using sediment samples from deep within sedimentary deposits [e.g., *Hancock et al.*, 1999; *Repka et al.*, 1997; *Schaller and Ehlers*, 2006] or sediment from active river channels [e.g., *Brown et al.*, 1998; *Hetzel et al.*, 2002]. Sediment deposits cannot be considered stable and possible degradation of deposits (e.g., denudation, burial, bioturbation, and cryoturbation) must be accounted for [e.g., *Brown et al.*, 1998]. Information about deposition age and denudation can be gained from analysis of cosmogenic nuclides in samples collected at different depths [e.g., *Granger and Smith*, 2000; *Phillips et al.*, 2000; *Shanahan and Zreda*, 2000b; *Siame et al.*, 2004; *Wolkowinsky and Granger*, 2004]. Mixing of the surface layer [e.g., *Brown et al.*, 1995] also influences the age determination and thus needs to be taken into account when soils are mixed [e.g., *Lal and Chen*, 2005, 2006; *Perg et al.*, 2001].

[4] In this study, ~1.5 m depth profiles from the Pinedale (independent age constraint is ~21 ka) and Bull Lake moraines (independent age constraint is ~140 ka) of the Fremont Lake area (Wyoming, United States) are analyzed for in situ–produced cosmogenic ^{10}Be to determine ages and denudation rates of moraine surfaces (Figure 1). We make use of the approach outlined by *Lal and Chen* [2005, 2006] which is based on the nuclide concentrations in a completely

[1]Department of Geological Sciences, University of Michigan, Ann Arbor, Michigan, USA.
[2]International School of Stavanger, Hafrsfjord, Norway.

0148-0227/09/2007JF000921

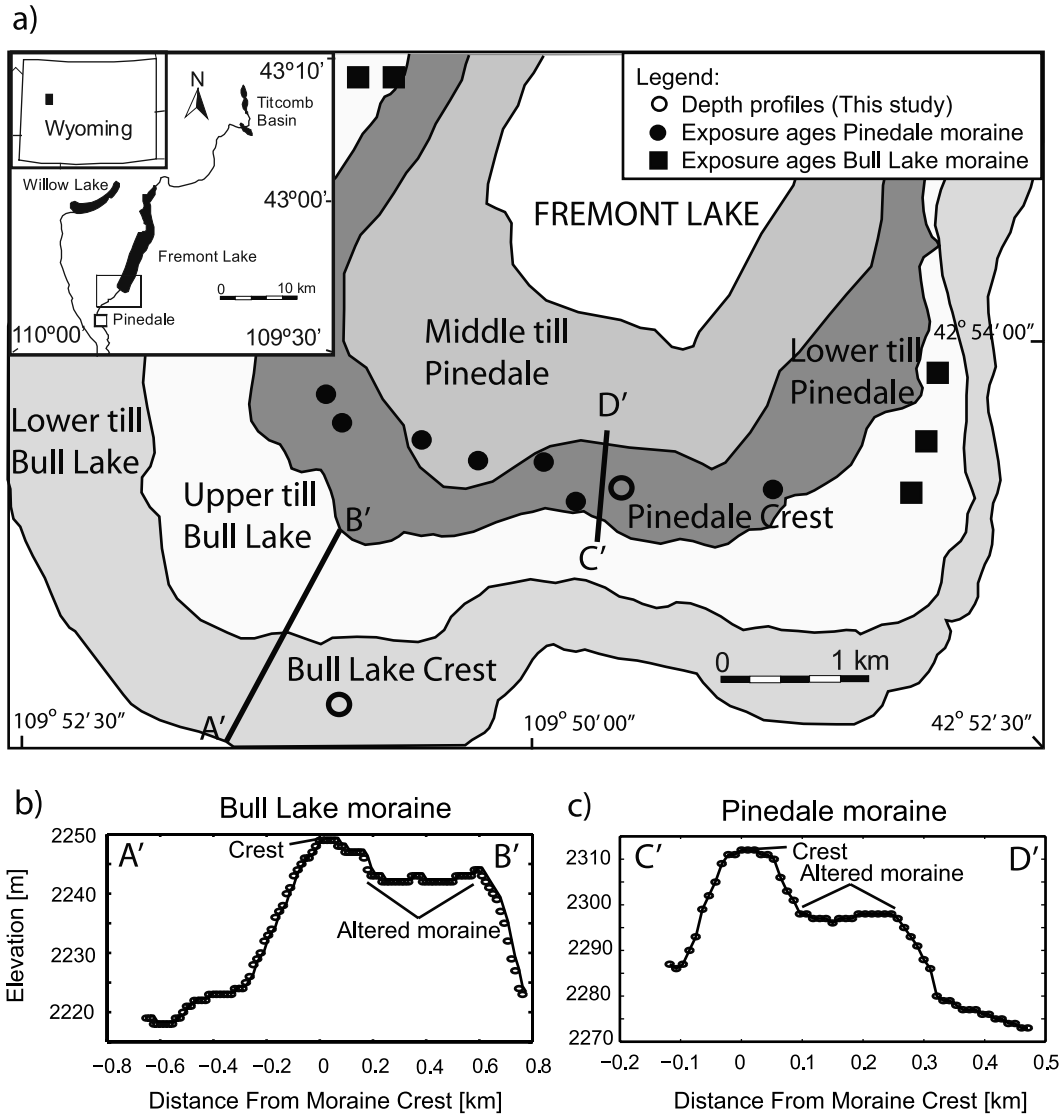

Figure 1. (a) Map showing location of depth profiles for cosmogenic nuclide analysis (open circles) taken from the terminal Pinedale (independent age constraint is ~21 ka) and Bull Lake (independent age constraint is ~140 ka) moraines in the Fremont Lake area, Wyoming (after *Richmond* [1973]). Also shown are locations of boulder surface exposure dates for Pinedale (solid circles) and Bull Lake (solid squares) moraines from *Gosse et al.* [1995] and *Phillips et al.* [1997]. See *Richmond* [1987] for a more detailed geologic map of the region. (b) Profile through the Bull Lake moraine based on 10 m digital elevation model. (c) Profile through the Pinedale moraine.

mixed surface layer and undisturbed depth section for age and denudation rate determination (Figure 2). We augment the complete mixing approach of *Lal and Chen* [2005, 2006] and also consider the effect of partial mixing on nuclide concentrations (Figure 2b). We compare these results to age and denudation rate determinations based on the measurement of several samples in the depth profile. This comparison is conducted to evaluate if two or multiple samples in the profile are required for age and denudation rate determinations. Ages and denudation rates from depth profiles are determined with Chi-square analysis of measured and modeled nuclide concentrations. The modeled nuclide concentrations take into account mixing in the surface layer and nuclide inheritance. Denudation of the moraine is addressed with the following two scenarios: (1) constant denudation of the moraine and (2) transient denudation of the moraine by hillslope diffusion. We compare the results to independent age constraints available for Pinedale and Bull Lake moraines and to denudation rates of moraines available from the literature. Possible problems in applying the method of *Lal and Chen* [2005, 2006] and the depth profile technique to our samples and elsewhere are discussed.

2. Background

2.1. Study Area

[5] The Fremont Lake area was glaciated by large valley glaciers extending from the highland ice caps covering the

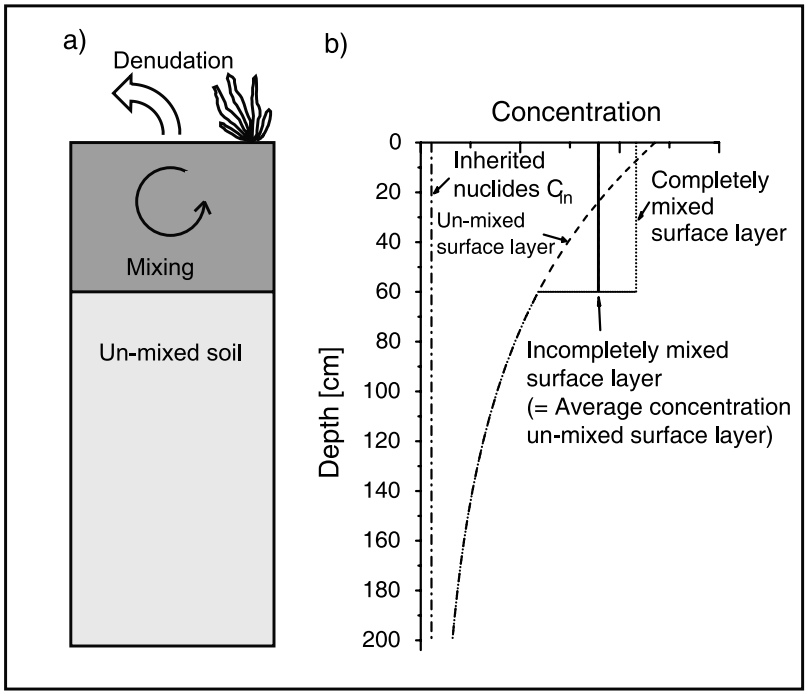

Figure 2. (a) Schematic sketch of a soil profile undergoing denudation and soil mixing to a given depth. (b) Possible nuclide concentration in a soil profile subjected to the different processes as shown in Figure 2a. The nuclide concentration of an unmixed layer (dashed line), the average nuclide concentration of this unmixed layer down to the assumed mixing depth (bold line), the nuclide concentration in a completely mixed surface layer (dotted line), and the inherited nuclide concentration (dotted-dashed line) are shown.

Wind River Mountains (Wyoming, United States). Several glaciations are documented in the Fremont Lake area including the Pinedale, Bull Lake and possibly the Sacagawea glaciations (Figure 1 [*Richmond*, 1973]). Several moraines from the Pinedale (1–7) and Bull Lake (I–V) glaciations were mapped in detail by *Richmond* [1987] with "1" and "I" designated as the terminal moraines. The moraines are composed of till which is a mixture of Archean granite, granodiorite, and diorite gneiss. The primary minerals observed in unweathered till (soil parent material) include plagioclase, quartz, biotite, K-feldspar, hornblende, and magnetite (by decreasing abundance). Quartzite cobbles found in the lower till of the Bull Lake moraines are attributed to reworking of older terrace deposits [*Richmond*, 1973].

[6] Pinedale moraines are steep sided with many boulders at the surface, whereas Bull Lake moraines have gentler slopes and fewer boulders. Soils on the Pinedale and Bull Lake moraines have been extensively studied [e.g., *Dahms*, 2002, and references therein]. Soils on Pinedale moraines have an average solum thickness of 38 cm whereas Bull Lake moraines have an average solum thickness of at least 125 cm [*Hall and Shroba*, 1995]. The mean annual temperature and precipitation in the Fremont Lake area are 1.8°C and 231 mm, respectively [*Zimmerman et al.*, 1994; *Weather Bureau*, 1965]. The dominant vegetation on the terminal moraines in the Fremont Lake area is big mountain sagebrush (*Artemisia tridentata*), which has been in the area since at least 11.5 ka as determined by ^{14}C [*Barnosky et al.*, 1987].

2.2. Previous Moraine Age Constraints

[7] Age determinations of moraines in the Fremont Lake area are based on cosmogenic nuclide exposure ages of boulders. In this section, the ages of the moraines from the Fremont Lake area are compared to age constraints of Pinedale and Bull Lake moraines from other locations in the Rocky Mountains (Wyoming and Colorado). A best age estimate, independent from the depth profile analysis of this study, is presented for the Pinedale and Bull Lake moraines.

[8] Boulders from Pinedale moraines in the Fremont Lake area are exposure age dated with ^{10}Be at 21.7 ± 0.7 ka [*Gosse et al.*, 1995]. A recalculated mean age based on data presented by *Gosse et al.* [1995], but using different production rates is 19.6 ka [*Benson et al.*, 2005]. Boulders from Bull Lake moraines in the Fremont Lake area reveal ^{10}Be exposure ages ranging from 115 to 160 ka with a mean age of 140 ka [*Easterbrook et al.*, 2003]. The youngest Bull Lake moraine at Fremont Lake (Moraine V after *Richmond* [1987]) was also attributed a combined $^{10}Be/^{36}Cl$ age of 113 ka [*Phillips et al.*, 1997].

[9] Boulder surface exposure ages of Pinedale moraines from northcentral and southwestern Colorado based on ^{36}Cl analysis range between 16 and 23 ka [*Benson et al.*, 2004, 2005]. Taking into account the effect of Holocene or Late Pleistocene instead of present-day snow shielding results in ages which are on average 2.2 ka older [*Benson et al.*, 2004]. Other cosmogenic age constraints for Pinedale moraines in the Bull Lake area, Wind River Mountains, indicate an age range of 16–23 ka [*Phillips et al.*, 1997;

Zreda and Phillips, 1995] and ^{230}Th/U dating of pedogenic carbonate from Pinedale age terraces in the Wind River Basin suggest that they formed at 21 ± 5.1 ka [*Sharp et al.*, 2003]. End moraines marking the Pinedale position in the Yellowstone glacial system range from 18.8 ± 0.9 to 16.5 ± 1.4 ^{10}Be ka [*Licciardi and Pierce*, 2008]

[10] Many boulder ages from different localities in the Rocky Mountains indicate Bull Lake glaciation ages ranging from 90 to 150 ka [e.g., *Benson et al.*, 2004; *Licciardi and Pierce*, 2008; *Phillips et al.*, 1997]. Age constraints by ^{230}Th/U dating of pedogenic carbonate in terraces from the Wind River Basin formed contemporaneously with the Bull Lake moraines indicate an age of 150 ± 8.3 ka [*Sharp et al.*, 2003]. The Bull lake glaciation is therefore thought to be nearly synchronous with the maximum global ice volume of marine isotope stage 6 [*Sharp et al.*, 2003]. Many surface exposure ages of boulders from Bull Lake moraines are considered to be minimum ages for the glaciation age due to denudation of boulder surfaces, spallation during bush fires, denudation of the matrix material and snow shielding [e.g., *Benson et al.*, 2004]. In summary, we consider ages of 21 and 140 ka to be the independent best age estimates for the formation of the Pinedale and Bull Lake terminal moraines in the Fremont Lake area, Wyoming. These independent age constraints are used for comparison to ages determined in this study.

2.3. Previous Moraine Denudation Constraints

[11] Several studies have recently suggested that postdepositional moraine denudation may be more substantial than previously thought. The different studies, which we summarize below, are based on (1) field observations, (2) diffusion models of surface degradation and moraine boulder frequency analysis, (3) exhumation modeling of boulder surface exposure ages with in situ–produced cosmogenic nuclides, and (4) depth profile dating with in situ–produced cosmogenic nuclides. In order to allow a comparison between the different techniques, we translate the net denudation reported from field observations and diffusion models into constant denudation rates (approximate values given in parenthesis).

2.3.1. Field Observations

[12] In the upper Colorado River Basin, ten profiles of Bull Lake and Pinedale moraines were surveyed [*Meierding*, 1984] and results suggest the Bull Lake moraines lost ~10 m more material than the Pinedale moraines since deposition. Boulder age considerations for Bull Lake moraines suggest <1 m (~0.005 mm a^{-1}) was removed in the western part of the Wind River Mountains and >1.4 m (~0.010 mm a^{-1}) of material was removed in the eastern part of the Wind River Mountains [*Easterbrook et al.*, 2003]. No obvious correlation between the boulder height and age were found for Bull Lake moraines on the western side of the Wind River Mountains, Wyoming [*Easterbrook et al.*, 2003]. The boulders which are all taller than 1 m have apparently always been exposed since their deposition. In contrast, boulders in the eastern side of Wind River Mountains show a correlation of boulder age and height. A 1.4 m tall boulder reveals a very young age (65 ka) in comparison to a 4 m tall boulder with an age of 130 ka [*Easterbrook et al.*, 2003]. Further field observations are summarized by *Putkonen and O'Neal* [2006].

2.3.2. Diffusion Models of Surface Degradation and Moraine Surface Boulder Frequency Analysis

[13] Diffusion models of surface degradation have been applied to lateral moraines in the Sierra Nevada, California, and suggest 16 m of surface lowering for the 22 ka old Tioga moraine (~0.70 mm a^{-1}) and 28 m of surface lowering for a 100 ka old moraine (~0.28 mm a^{-1} [*Hallet and Putkonen*, 1994]). The models assume a deposition angle of 31° and suggest that large moraines were lowered from 100 to 66 m in 100 ka (~0.34 mm a^{-1}) and small moraines from 20 to 10 m in 20 ka (~0.50 mm a^{-1} [*Putkonen and Swanson*, 2003]). The maximum depth of eroded material is considered to be ~25% of the final height of a moraine [*Putkonen and O'Neal*, 2006]. Applied to the 22 ka old lateral Tioga moraine with a height of ~45 m (used from *Hallet and Putkonen* [1994]) approximately 11 m of moraine material was suggested to have been eroded (~0.50 mm a^{-1}). Assuming an initial constant boulder frequency, surface lowering and related exhumation to the moraine surface can be determined [*Putkonen et al.*, 2008].

2.3.3. Exhumation Modeling of Boulder Surface Exposure Ages

[14] Exhumation modeling of boulder surface exposure ages produces a range of possible true landform ages and soil denudation rates [e.g., *Shanahan and Zreda*, 2000a; *Zreda et al.*, 1994]. Denudation rates of 0.025–0.037 mm a^{-1} were determined with cosmogenic ^{36}Cl for a 135–165 ka old moraine situated in Bishop Creek, Sierra Nevada [*Phillips et al.*, 2008]. Slower denudation rates of 0.015–0.018 mm a^{-1} and 0.005–0.007 mm a^{-1} were determined in 254–284 ka and 353–419 ka old moraines on Mount Kenya [*Shanahan and Zreda*, 2000b].

2.3.4. Depth Profile Dating

[15] Constant denudation rates of 0.020–0.060 mm a^{-1} were determined with ^{36}Cl and ^{10}Be for moraines from Bishop Creek, Sierra Nevada [*Shanahan and Zreda*, 2000a]. Similar rates (0.025 and 0.045 mm a^{-1}) were reported for the older Tahoe moraine (145 ka) and the Mono Basin moraine (85 ka) in Bloody Canyon, Sierra Nevada [*Phillips et al.*, 2000].

3. Depth Profile Sample Locations and Characteristics

[16] Depth profiles for in situ–produced cosmogenic ^{10}Be analysis were collected from the Pinedale terminal moraine (2298 m above sea level (asl), 42° 53′ 26″ N, 109° 49′ 34″ W) and the Bull Lake terminal moraine (2285 m asl, 42° 52′ 39″ N, 109° 51′ 00″ W) in the Fremont Lake area, Wyoming (Figure 1). The depth profiles are situated in the lower till of the Pinedale and Bull Lake moraines, respectively. Fourteen samples collected in ~15 cm intervals to a depth of 180 cm were obtained from the crest of the Pinedale terminal moraine. The depth profile from the crest position of the Bull Lake terminal moraine consists of 12 samples taken in ~10 cm intervals to a depth of 130 cm. The grain size distribution of the <2 mm size fraction was determined on 30 g of material. After removal of organic matter with hydrogen peroxide, the silt and clay fractions (<0.063 mm) were separated by wet sieving from the sand fraction. The relative percentage of the silt and clay frac-

Table 1. Grain Size Distribution and ^{10}Be Concentrations in Depth Profiles of the Pinedale and Bull Lake Moraines

Sample[a]	Soil Classification	Depth (cm)	Grain Size Analysis (<2 mm)[b] Sand (wt %)	Silt (wt %)	Clay (wt %)	^{10}Be Concentration[c] (10^5 atoms g^{-1})
Pinedale Moraine (2298 m asl, 42° 53′ 26″ N, 109° 49′ 34″ W)						
04-WRMP-014(E)	A horizon	3 ± 2	75	18	6	3.67 ± 0.14
04-WRMP-013(E)	B-horizon	10 ± 5	68	22	10	3.73 ± 0.09
04-WRMP-012(E)	B-horizon	20 ± 10	70	23	7	3.60 ± 0.15
04-WRMP-011(E)	B-horizon	30 ± 10	74	22	4	3.60 ± 0.08
04-WRMP-010	C-horizon	43 ± 10	76	19	5	
04-WRMP-009(E)	C-horizon	58 ± 10	82	15	3	2.44 ± 0.07
04-WRMP-008	C-horizon	73 ± 10	85	12	3	
04-WRMP-007(E)	C-horizon	88 ± 10	81	16	3	1.89 ± 0.09
04-WRMP-006	C-horizon	103 ± 10	82	15	3	
04-WRMP-005	C-horizon	118 ± 10	71	23	6	
04-WRMP-004(E)	C-horizon	133 ± 10	71	24	5	1.11 ± 0.03
04-WRMP-003	C-horizon	148 ± 10	74	21	6	
04-WRMP-002	C-horizon	163 ± 10	72	22	6	
04-WRMP-001	C-horizon	180 ± 10	72	23	6	
Bull Lake Moraine (2285 m asl, 42° 52′ 39″ N, 109° 51′ 00″ W)						
AT-FL-4L(E)	A horizon	5 ± 2	69	22	9	14.9 ± 0.9
AT-FL-4K(E)	A horizon	20 ± 5	51	29	20	14.8 ± 0.7
AT-FL-4J(E)	A horizon	28 ± 5	52	34	14	14.0 ± 0.6
AT-FL-4I(E)	Bk-horizon	43 ± 5	47	23	30	13.6 ± 0.8
AT-FL-4I(F)	Bk-horizon	43 ± 5				10.9 ± 0.6
AT-FL-4H	Bk-horizon	53 ± 5	50	28	22	
AT-FL-4G(E)	Bk-horizon	64 ± 5	54	26	20	9.08 ± 0.56
AT-FL-4F(E)	Bk-horizon	79 ± 10	60	24	16	8.50 ± 0.48
AT-FL-4E	Bk-horizon	89 ± 10	62	24	14	
AT-FL-4D	Bk-horizon	94 ± 10	75	17	9	
AT-FL-4C(E)	Bk-horizon	104 ± 10	64	26	10	6.65 ± 1.02
AT-FL-4C(F)	Bk-horizon	104 ± 10				5.69 ± 0.32
AT-FL-4C(G)	Bk-horizon	104 ± 10				5.50 ± 0.54
AT-FL-4B	Bk-horizon	114 ± 10	60	25	15	
AT-FL-4A(E)	Bk-horizon	130 ± 10	60	25	15	4.93 ± 0.28

[a]Letter in paranthesis indicates grain size analyzed for cosmogenic nuclides: E is 0.5–1.0 mm, F is 0.25–0.5 mm, and G is 0.125–0.25 mm.
[b]Grain size analysis as described in text.
[c]The ^{10}Be concentration in quartz corrected for blank, reported error includes analytical uncertainties (1 σ).

tions was determined by the settling method based on Stokes' law [e.g., *Day*, 1965].

[17] The depth profile of the Pinedale moraine has a sand content ranging from 68 to 85 wt %, a silt content ranging from 15 to 24 wt %, and a clay content ranging from 3 to 10 wt % (Table 1 and Figure 3a). The soil is a Cryoboroll with an A-horizon to ~5 cm depth and a B-horizon to 35 cm depth. At about 100 cm depth, there is a layer of cobbles and

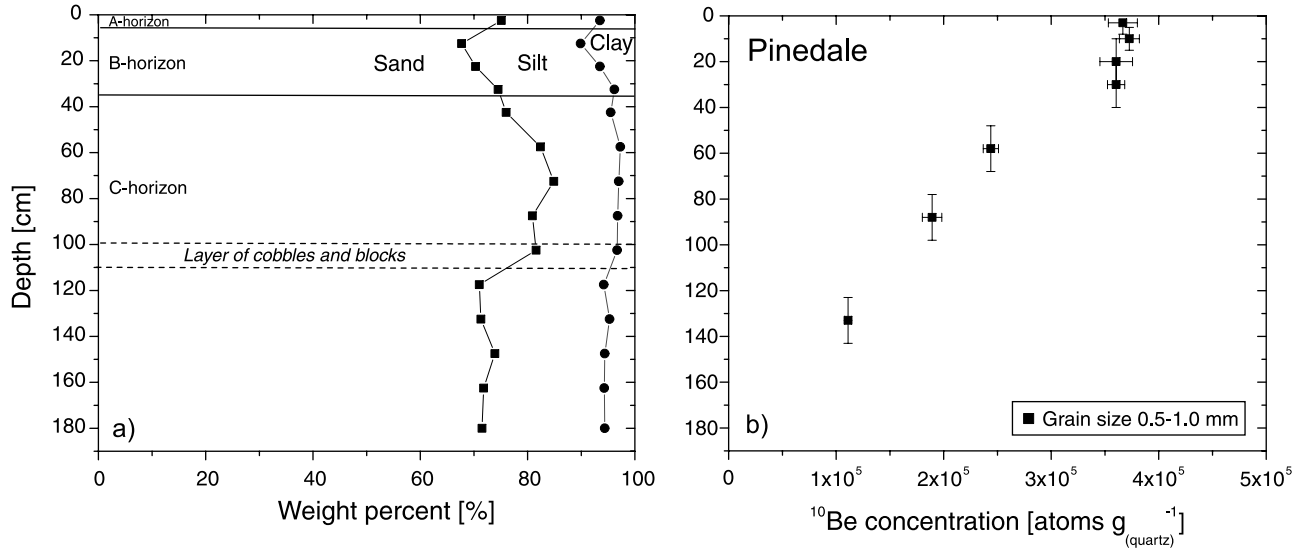

Figure 3. Depth profile for the Pinedale terminal moraine. (a) Grain-size distribution of the <2 mm fraction to a depth of 180 cm. (b) The ^{10}Be concentration measured in quartz from seven samples selected from the depth profile. The 0.5–1.0 mm grain-size fraction was analyzed.

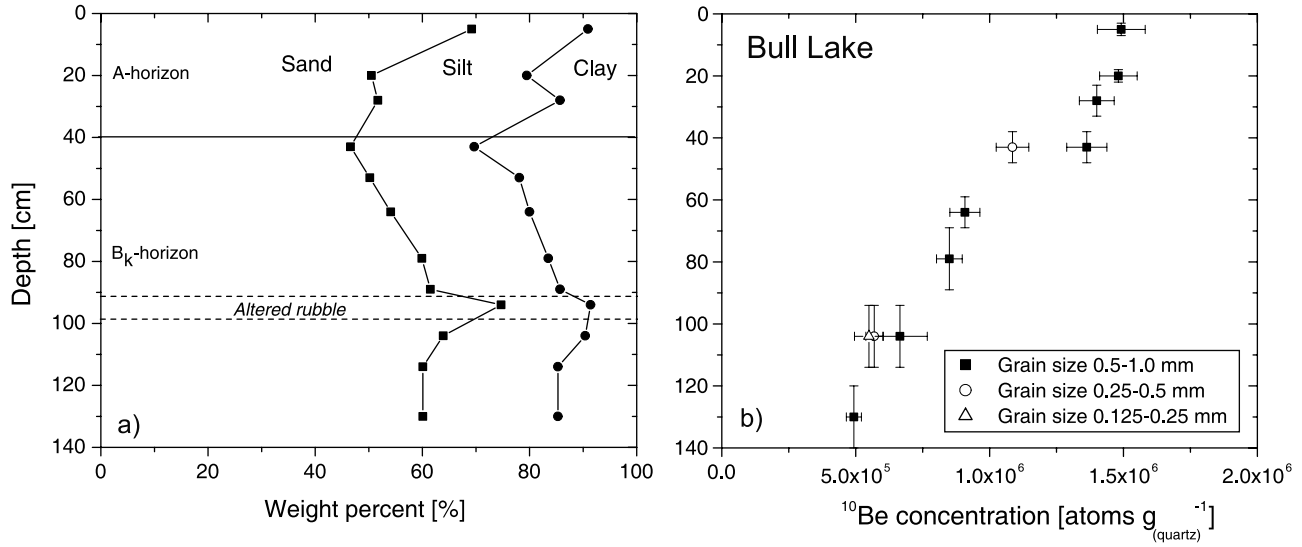

Figure 4. Depth profile in the Bull Lake terminal moraine. (a) Grain-size distribution of the <2 mm fraction to a depth of 130 cm. (b) The ^{10}Be concentration measured in quartz from eight samples of the 0.5–1.0 mm grain size fraction. Additional grain sizes have been analyzed for samples from 43 to 104 cm depth.

boulders. Above this layer the silt content generally decreases and the sand content increases with depth. Below the layer of cobbles and boulders the silt and sand contents remain constant (21–24 wt % and 71–74 wt %, respectively).

[18] In the Bull Lake depth profile, the sand content ranges from 47 to 75 wt %, the silt content from 17 to 34 wt %, and the clay content from 9 to 30 wt % (Table 1 and Figure 4a). The clay content increases to its highest value of 30 wt % at 43 cm depth. This soil is also a Cryoboroll with an A-horizon to ~30 cm. The depth of the B-horizon is not observed, but estimated at 125 cm on the basis of *Hall and Shroba* [1993]. However, we note that the delineation of soil horizons in these very weakly developed soils is difficult and somewhat subjective.

4. Methods

[19] We make use of two different approaches to determine ages and denudation rates based on cosmogenic nuclide measurements. Approach A uses the principles presented by *Lal and Chen* [2005, 2006]. Approach B presents an alternative approach to the analytic solution of Lal and Chen and calculates ages and denudation rates based on a Chi-square analysis of measured depth profiles. We start by describing our cosmogenic sample analysis procedures.

4.1. Cosmogenic Nuclide Analysis

[20] Seven samples of the Pinedale and eight samples of the Bull Lake depth profiles were selected for the analysis of in situ–produced ^{10}Be (Figures 3b and 4b and Table 1). Approximately 15–120 g and 5–15 g of pure quartz were separated from the 0.5 to the 1.0 mm grain size fraction for the Pinedale and Bull Lake profiles, respectively. For two samples of the Bull Lake depth profile (AT-FL-4C and I) different grain size fractions (0.125–0.25 mm, 0.25–0.5 mm) were analyzed in order to test grain size variability of the cosmogenic nuclide concentration. The basic technique used in this study to separate ^{10}Be is described by *von Blanckenburg et al.* [1996]. Cosmogenic nuclide ratios were measured at the accelerator mass spectrometer facility of PRIME Lab, Purdue University. Data are referenced to the original ICN standard. Nuclide concentrations were corrected for machine as well as chemistry blanks. The reported standard error includes analytical uncertainties (1σ).

4.2. Age and Denudation Rate Determination

4.2.1. Approach A: The Lal and Chen Approach

[21] The approach of Lal and Chen is based on the assumption that the age and denudation rate of a sedimentary deposit can be determined by measuring one sample from the mixed surface layer and another sample from the undisturbed layer below the mixed layer [*Lal and Chen*, 2005, 2006]. The age and denudation rate calculations are based on two independent equations and as long as the upper layer is reasonably well mixed an estimate of the age and denudation rate can be determined. For an undisturbed moraine eroding at a constant denudation rate D [cm a^{-1}], the calculated nuclide concentration C_{calc} [atoms g$_{(\mathrm{qtz})}^{-1}$] for a certain depth x [cm] is given by

$$C_{\mathrm{calc}}(x) = C_{\mathrm{in}} e^{(-\lambda t)} + P_{\mathrm{nuc}}(0)\frac{a_{\mathrm{nuc}}\mathrm{SCF}_{\mathrm{nuc}} e^{\left(-\frac{\rho x}{b_{\mathrm{nuc}}}\right)}}{\left(\lambda + \frac{\rho D}{b_{\mathrm{nuc}}}\right)}\left(1 - e^{\left(-t\left(\lambda + \frac{\rho D}{b_{\mathrm{nuc}}}\right)\right)}\right) + P_{\mu\mathrm{stopped}}(0)\sum_{j=1}^{3}\frac{a_j \mathrm{SCF}_j e^{\left(-\frac{\rho x}{b_j}\right)}}{\left(\lambda + \frac{\rho D}{b_j}\right)}\left(1 - e^{\left(-t\left(\lambda + \frac{\rho D}{b_j}\right)\right)}\right) + P_{\mu\mathrm{fast}}(0)\sum_{k=1}^{3}\frac{a_k \mathrm{SCF}_k e^{\left(-\frac{\rho x}{b_k}\right)}}{\left(\lambda + \frac{\rho D}{b_k}\right)}\left(1 - e^{\left(-t\left(\lambda + \frac{\rho D}{b_k}\right)\right)}\right), \quad (1)$$

Table 2. Snow Shielding Factors for Model Calculations

Index	a[a]	b[b] (g cm^{-2})	SCF[c]
	Nucleonic Production		
	1	157	0.925
	Stopped Muonic Production		
$j = 1$	0.845	1030	0.988
$j = 2$	−0.05	160	0.926
$j = 3$	0.205	3000	0.996
	Fast Muonic Production		
$k = 1$	0.01	100	0.887
$k = 2$	0.615	1520	0.992
$k = 3$	0.375	7600	0.993

[a]Dimensionless coefficient for depth scaling of the surface production rate as used by *Schaller et al.* [2002]. The nucleonic depth dependence is exponential (see text).

[b]Coefficient for depth scaling of the surface production rate as used by *Schaller et al.* [2002] except for the nucleonic production. Here b should not be considered as real mean absorption path, but as parameter of the complex depth function into an exponential format.

[c]Snow correction factor for present-day snow cover based on snow depths from Elkhard pass SNOTEL station.

where C_{in} [atoms $g_{(qtz)}^{-1}$] is the inherited nuclide concentration assumed to be constant with depth, λ [years^{-1}] is the decay constant, t [years] is the time since moraine deposition, ρ [g cm^{-3}] is the density of the till, and $P_{nuc}(0)$, $P_{\mu stopped}(0)$, and $P_{\mu fast}(0)$ are the local surface production rates [atoms $g_{(qtz)}^{-1}$ a^{-1}] by nucleons, stopped and fast muons, respectively. The coefficients $a_{nuc,j,k}$ [dimensionless] and $b_{nuc,j,k}$ [g cm^{-2}] are for the depth scaling of the production rate (Table 2, see also *Schaller et al.* [2001, 2002] for more details). SCF [dimensionless] is the snow correction factor to correct the production rate at the soil surface for present-day snow cover (see below).

[22] In a soil, where the surface layer is mixed, the nuclide concentration of samples below the mixed surface layer can still be calculated using equation (1). The mixing depth x_{Bio} [cm] is considered to be constant. The nuclide concentration in a reasonably well-mixed surface layer can be expressed by

$$C_{calc}(x) = C_{in}e^{(-\lambda t)} + \left(\frac{b_{nuc}e^{\left(-\frac{\rho x_{Bio}}{b_{nuc}}\right)}}{b_{nuc} - \rho x_{Bio}}\right) \cdot \left[P_{nuc}(0)\frac{a_{nuc}SCF_{nuc}}{\left(\lambda + \frac{\rho D}{b_{nuc}}\right)}\left(1 - e^{\left(-t\left(\lambda + \frac{\rho D}{b_{nuc}}\right)\right)}\right)\right] + \left(1 - \frac{b_{nuc}e^{\left(-\frac{\rho x_{Bio}}{\Lambda}\right)}}{b_{nuc} - \rho x_{Bio}}\right)\left[P_{nuc}(0)\frac{a_{nuc}SCF_{nuc}}{\left(\lambda\frac{\rho x_{Bio}}{b_{nuc}} + \frac{\rho D}{b_{nuc}}\right)} \cdot \left(1 - e^{\left(-t\left(\lambda + \frac{D}{x_{Bio}}\right)\right)}\right)\right]. \quad (2)$$

[23] For simplicity equation (2) is only written for the nucleonic production. However, the stopped and fast muonic productions need to be accounted for as addressed in equation (1). Equation (2) follows equation (5) by *Brown et al.* [1995] rather than equation (12) by *Lal and Chen* [2005, 2006]. For age and denudation rate determination, the ratio of the concentration in the mixed layer and the undisturbed layer are plotted versus the concentration in the mixed layer (see Figure 5).

[24] In our study, a soil reflecting the nuclide concentration as calculated with equation (2) is considered to be completely mixed (Figure 2). In contrast, a surface layer is considered incompletely mixed when it does not reflect the nuclide concentration as calculated with equation (2). This incomplete mixing might be the result of recent mixing, different mixing depths, or depth-dependent mixing.

[25] Details of our calculations are as follows: For calculations, we use sea level high-latitude production rates of 5.1 atoms $g_{(qtz)}^{-1}$ a^{-1} for the total production rate [*Stone*, 2000] resulting in 4.9 atoms $g_{(qtz)}^{-1}$ a^{-1} for nucleonic, 0.106 atoms $g_{(qtz)}^{-1}$ a^{-1} for stopped muonic, and 0.093 atoms $g_{(qtz)}^{-1}$ a^{-1} for fast muonic production rates [*Heisinger et al.*, 2002a, 2002b]. The sea level high-latitude values were scaled to the sample altitude and latitude using scaling factors of *Dunai* [2000]. The depth dependence of the nucleonic production is exponential and has an absorption mean free path a_{nuc} = 157 g cm^{-2} (see Table 2). The depth dependence of stopped and fast muonic production is as determined by *Schaller et al.* [2002]. The decay constant for ^{10}Be used is 4.62 × 10^{-7} years^{-1}. No variations in the production rate due to changes in the geomagnetic field intensity are applied [*Masarik et al.*, 2001]. The density of the moraine deposit is approximately 2.0 g cm^{-3} [*Taylor and Blum*, 1995] with an uncertainty of ±0.4 g cm^{-3}. Soil mineral dissolution has not been taken into account as dissolution rates and their change are difficult to constrain over time. The incorporation of loess (grain size range is 0.015–0.05 mm) has also not been modeled as loess addition is considered to be minor in the Fremont Lake area [*Hall and Shroba*, 1993].

[26] The production rate scaled from sea level high latitude to the sample altitude and latitude needs to be corrected for reduction by snow cover. The monthly snow water equivalents of a 30 years record of data from the nearby Elkhard Pass, SNOTEl station (2860 m asl) has been used to calculate the present-day snow correction factor SCF for the production rate [e.g., *Benson et al.*, 2004; *Gosse and Phillips*, 2001; *Schildgen et al.*, 2005]. The SCFs have been determined for each production mechanism (nucleonic, stopped and fast muonic). As we use the depth dependence of *Schaller et al.* [2002] for the stopped and fast muonic production, we need to determine the SCF for the six different production mechanisms (Table 2).

4.2.2. Approach B: Chi-Square Analysis of Cosmogenic Nuclide Concentrations

[27] In our second approach we use a Chi-square analysis to compare the measured nuclide concentrations to predicted concentrations using a numerical model. The numerical model calculates nuclide concentrations based on different assumption of age, denudation rate, mixing depth, and inherited nuclide concentration. The Chi-square analysis is based on three components which are presented below.

4.2.2.1. Modeled Cosmogenic Nuclide Concentration

[28] We use a numerical model to calculate the ^{10}Be concentration at each sample depth. The concentration is calculated as a function of age, denudation rate of the moraine, the inherited nuclide concentration, the mixing depth, the production rate at the sample locality, the snow correction factor, and the density of the till. All but the latter three are considered free parameters in the Chi-square analysis of this study. We take into consideration the

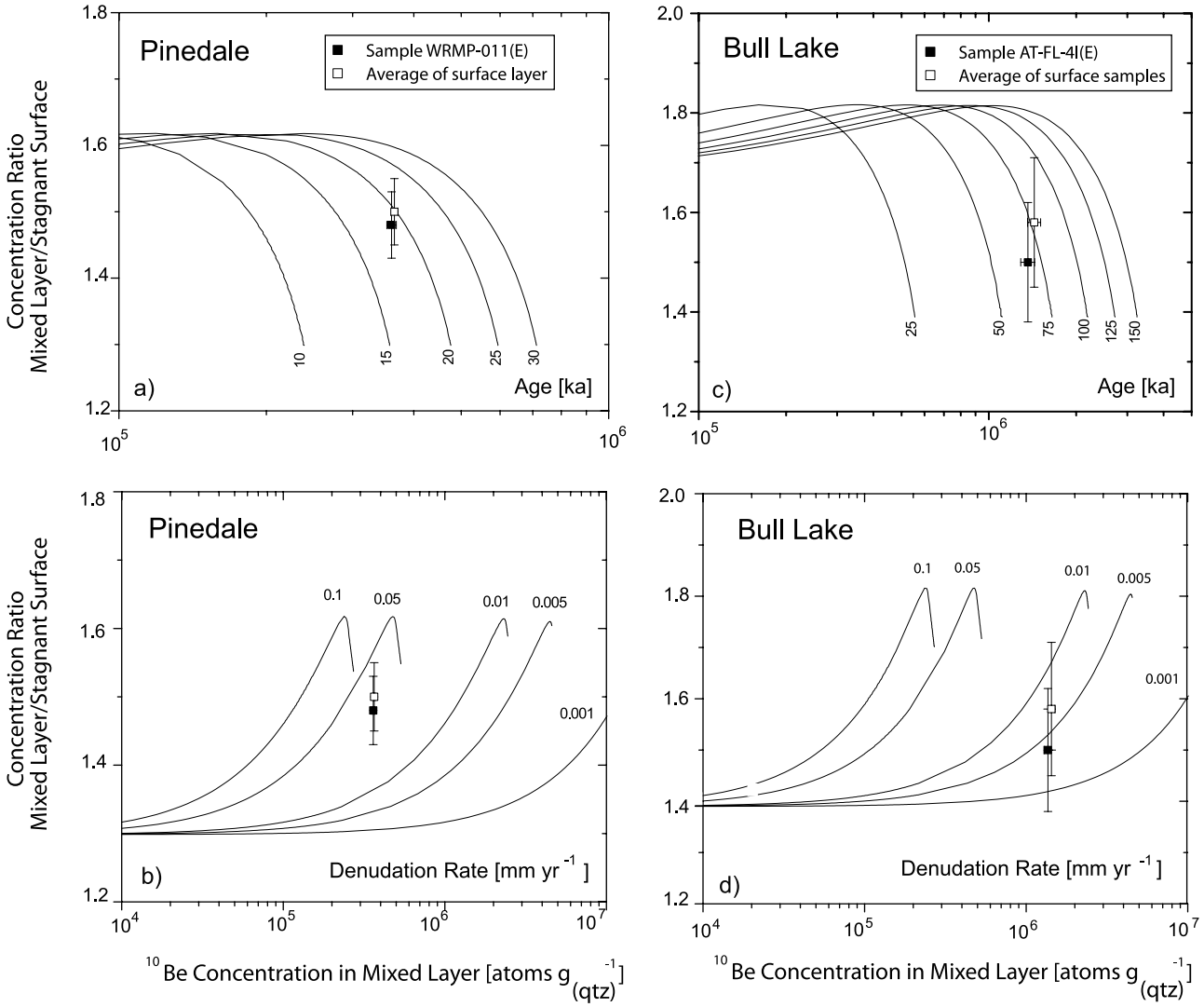

Figure 5. The ratio of the nuclide concentration in the mixed surface layer to the nuclide concentration of the uppermost sample in the unmixed layer is plotted versus the concentration in the surface layer as described by *Lal and Chen* [2005, 2006]. The nuclide concentration of the surface layer is based on the sample just above the mixing boundary (solid squares) or on the average nuclide concentrations of all samples in the surface layer (open squares). (a) Different age calculations are compared with measured values for the Pinedale moraine. The calculations are based on a mixing depth of 40 cm, production rates as used for the Chi-square analyses, and a density of 2.0 g cm^{-3}. (b) Different denudation rate calculations for the Pinedale moraine are compared with measured values. (c) Different age calculations are compared with measured values for the Bull Lake moraine. The calculations are based on a mixing depth of 50 cm, production rates as used for the Chi-square analyses, and a density of 2.0 g cm^{-3}. (d) Different denudation rate calculations for the Bull Lake moraine.

following two different denudation rate scenarios: (1) constant denudation rate over the time since moraine deposition and (2) transient denudation rate decreasing in magnitude over time since moraine deposition. The constant denudation rate scenario is considered to evaluate the usefulness of the simplest approach to interpreting the data compared to more sophisticated approaches (see section 6).

[29] In the case of constant denudation, the nuclide concentrations in the undisturbed layer and the mixed surface layer were calculated using equations (1) and (2). The four variables used as free parameters for the Chi-square analysis are age t, constant denudation rate of the moraine D, the inherited nuclide concentration C_{in}, and the mixing depth x_{Bio}. Three variables, which are not used as free parameters in our model calculations, influence the calculated nuclide concentration C_{calc}: the production rate $P(0)$ at the sample locality, the snow correction factor SCF, and the density ρ of the till. The production rate $P(0)$ is a variable due to uncertainties in the scaling from sea level to high altitude. The snow correction factor is a source of uncertainty due to the unknown shielding effect of snow cover over the time since moraine deposition. The density is a variable due to the unknown change of density over time

and the difficulty in accurately determining densities in deposits of coarse-grained sediments.

[30] In the case of transient denudation, equations (1) and (2) are not valid anymore. The nuclide concentration for a sample at a given depth needs to be calculated with a numerical model. This numerical model takes into account the changing denudation rate over given time intervals. The calculation of the transient denudation rate over time is based on the evolution of 1-D topographic profiles. We use the following 1-D transient diffusion equation for modeling moraine denudation, following the approach of *Fernandes and Dietrich* [1997]

$$\frac{dh}{dt} = k\frac{d^2h}{dy^2}, \tag{3}$$

where h [m] is the height of the moraine, k [m^2 a^{-1}] is the topographic diffusivity, and y [m] is horizontal distance. Equation (3) is solved using an explicit finite difference scheme. The intitial topographic geometry used for these simulations was a flat-topped moraine with sides at a constant slope. Free parameters considered in the initial condition include the half width and height of the flat top, and the deposition angle of the moraine sides. Model results from simulations with different parameter settings are compared to observed profiles at the sample locations. The observed profiles are based on 10 m digital elevation models (Figure 1). We note that alternative, nonlinear, diffusion models have been proposed for hillslope denudation of soil mantled bedrock [*Roering et al.*, 2001]. However, as demonstrated later the nuclide data lack sensitivity to either the constant or transient denudation histories and a more complicated analysis of hillslope denudation is not warranted.

[31] The cosmogenic nuclide concentration with depth in a moraine eroding under transient conditions is calculated with a numerical model. The nuclide concentration of samples from below the mixed layer is predicted by integrating the nuclide production at depth for given denudation rates over the time interval denudation occurs. The nuclide concentration C_{ave} in the mixed surface layer is calculated by the average production P_{ave} at each time interval, the input of nuclides from below the mixed layer for a given denudation rates at certain time intervals, as well as losses through denudation at the surface and radioactive decay at each time interval (see equation (4) and Appendix 1 of *Brown et al.* [1995])

$$\frac{dC_{ave_{nuc}}}{dt} = P_{ave_{nuc}} + \frac{D}{x_{Bio}}C_{x_{Bio}nuc} - \frac{D}{x_{Bio}}C_{ave_{nuc}} - \lambda C_{ave_{nuc}}, \tag{4}$$

where $C_{x\mathrm{Bio}nuc}$ [atoms $g^{-1}_{(qtz)}$] is the nuclide concentration in the material just below the mixed layer. $C_{x\mathrm{Bio}nuc}$ is calculated as described above. For simplicity, equation (4) is written for nucleonic production only, but needs to be extended for stopped and fast muonic production as shown in equation (1). The average nucleonic production rate in the mixed layer is calculated following equation (5) (see also Appendix 1 of *Brown et al.* [1995])

$$P_{ave_{nuc}} = P_{nuc}(0)\frac{a_{nuc}SCF_{nuc}}{\left(\frac{\rho x_{Bio}}{b_{nuc}}\right)}\left(1 - e^{\left(-\frac{\rho x_{Bio}}{b_{nuc}}\right)}\right). \tag{5}$$

The stopped and fast muonic production rates can be calculated following equation (1).

4.2.2.2. Chi-Square Statistical Analysis

[32] We determined combinations of model parameters that provide the best fit solutions for the data using a Chi-square statistical analysis. Our approach is comparable to that used in other studies [e.g., *Braucher et al.*, 2008; *Ehlers et al.*, 2003; *Siame et al.*, 2004; *Whipp et al.*, 2007; *Wolkowinsky and Granger*, 2004]. The range of values used for each parameter is presented in the next section. Calculated and measured ^{10}Be concentrations were compared for each profile using a reduced sum Chi-square statistical test

$$\chi^2 = \frac{\sum_{i=1}^{N}\left(\frac{C_{calc}(i) - C_{meas}(i)}{1\sigma_{meas}(i)}\right)^2}{N}, \tag{6}$$

where $C_{calc}(i)$ and $C_{meas}(i)$ are the calculated and the measured nuclide concentrations for a given sample (i), respectively, $1\sigma_{meas}(i)$ is the one sigma error of the measured nuclide concentration of sample (i), and N is the total number of samples. For each depth profile, reduced sum Chi-square analyses for age, constant and transient denudation of the moraine, nuclide inheritance, and mixing depth are based on all samples measured in the depth profile and assuming complete mixing or no mixing. We calculate the best reduced sum Chi-square solution for present-day snow shielding correction. Best fit combinations of parameters are identified as the values that produce the lowest reduced sum of Chi-square misfit. A misfit of 1 indicates a perfect fit to the data.

4.2.2.3. Range and Resolution of Parameters Used

[33] Our Chi-square analysis explored the effect of different ranges and resolutions of the parameters on depth profile concentrations from each moraine. The range of parameters explored in our analysis is as follows. The age range explored for the Pinedale moraine is 10–30 ka with an increment of 0.5 ka. Constant denudation rates of the moraine are between 0 and 0.1 mm a^{-1} allowing a step resolution of 0.0025 mm a^{-1}. Transient denudation rates are constrained by the hillslope diffusivity (see footnotes of Table 3), starting height of the moraine (20, 30, and 40 m), and deposition angle (5, 10, 15, 20, 25, and 30°). The range for the inherited nuclide concentration used is between 0 and 4×10^5 atoms g^{-1} with a step resolution of 0.2×10^5 atoms g^{-1}. The mixing depth range for the Pinedale moraine is 0–100 cm with a depth resolution of 10 cm. The allowed age range for the Bull Lake moraine is between 30 and 200 ka with an age resolution of 2.5 ka. Constant denudation rates of the moraine are allowed to be 0–0.05 mm a^{-1} with a resolution of 0.0025 mm a^{-1}. Transient denudation rates are constrained by diffusivity (see footnotes of Table 3), starting height of the moraine (35, 40, 50, and 60), and deposition angle (5, 10, 15, 20, 25, and 30°). The inherited nuclide concentration is between 0 and 4×10^5 atoms g^{-1} with a step resolution of 0.2×10^5 atoms g^{-1}. The mixing depth range for the Bull Lake moraine is 0–100 cm with a depth resolution of 10 cm.

5. Results

5.1. Measured Cosmogenic Nuclide Concentrations

[34] The ^{10}Be concentrations measured in quartz within the 0.5–1.0 mm grain size fraction are presented for the

Table 3. Best Chi-Square Solutions for Different Model Simulations Assuming Constant and Transient Denudation

Type of Denudation	Model	Samples Used	Age[a] (ka)	Average Denudation[b] (mm a^{-1})	Inheritance ^{10}Be Concentration[c] (10^5 atoms g^{-1})	Mixing Depth[d] (cm)	Diffusivity k[e] (10^{-3} m^2 a^{-1})	Maximum Height[f] (m)	Slope Angle[g] (degrees)	Chi-Square Value	Figure
Pinedale Moraine (2298 m asl, 42° 53′ 26″ N, 109° 49′ 34″ W)[h]											
Constant	1	all 7 samples	16.5–17.5	0.0–0.005	0.2	50				0.7–0.9	6
Constant	2	lower 3 samples	***21.0***	0.0175	0.2	0				0.7	
Transient	3	all 7 samples	17.0–24.0	0.003–0.051	0.2	40, 50	0.3–30	30, 40	20	0.5	7, 9
Transient	4	lower 3 samples	***21.0***	0.032–0.034	0.2	0	7.5–10	40	20, 25, 30	0.7–0.9	10
Bull Lake Moraine (2285 m asl, 42° 52′ 39″ N, 109° 51′ 00″ W)[i]											
Constant	5	all 8 samples	65.0–72.5	0.0–0.003	1.4–2.0	60				0.4–0.5	6
Constant	6	lower 4 samples	***140***	0.0100	1.4	0				0.3	
Transient	7	all 8 samples	70–127.5	0.0–0.016	1.4–1.6	50, 60	0.1–20	35, 40, 50, 60	5, 10, 15, 20, 25, 30	0.4	8, 9
Transient	8	lower 4 samples	***140***	0.010–0.022	1.0–1.4	0	0.4–30	35, 40, 50, 60	5, 10, 15, 20, 25, 30	0.3–0.4	10

[a]Age range and resolution: Pinedale 10–30 ka and 0.5 ka and Bull Lake 30–200 ka and 2.5 ka. Values in bold italics have no free parameters.
[b]Denudation rate range and resolution for constant denudation: Pinedale 0–0.1 mm a^{-1} and 0.0025 mm a^{-1} and Bull Lake 0–0.05 mm a^{-1} and 0.0025 mm a^{-1}. For the transient denudation the range of the average denudation rate is given by diffusivity k, max h, and slope angle.
[c]Inherited nuclide concentration range and resolution: Pinedale and Bull Lake 4×10^5 atoms $g_{(qtz)}^{-1}$ and 0.2×10^5 atoms $g_{(qtz)}^{-1}$.
[d]Mixing depth range and resolution: Pinedale and Bull Lake 0–100 cm and 10 cm.
[e]Diffusivities for Pinedale and Bull Lake are 0.075×10^{-3}, 0.1×10^{-3}, 0.15×10^{-3}, 0.2×10^{-3}, 0.25×10^{-3}, 0.3×10^{-3}, 0.4×10^{-3}, 0.5×10^{-3}, 0.75×10^{-3}, 1×10^{-3}, 2×10^{-3}, 3×10^{-3}, 4×10^{-3}, 5×10^{-3}, 10×10^{-3}, 25×10^{-3}, and 50×10^{-3} m^2 a^{-1}.
[f]The maximum heights for the Pinedale moraine are 20, 30, and 40 m, whereas for the Bull Lake they are 35, 40, 50, and 60 m.
[g]Slope angle range for Pinedale and Bull Lake from 5–30°. The resolution is 5° steps.
[h]Nucleonic production rate $P_n = 29.84$ atoms $(g_{(qtz)}\ a)^{-1}$, stopped muonic production rate $P_{\mu stop} = 0.294$ atoms $(g_{(qtz)}\ a)^{-1}$ and fast muonic production rate $P_{\mu fast} = 0.105$ atoms $(g_{(qtz)}\ a)^{-1}$. Production rates are not corrected for snow shielding.
[i]Nucleonic production rate $P_n = 29.56$ atoms $(g_{(qtz)}\ a)^{-1}$, stopped muonic production rate $P_{\mu stop} = 0.293$ atoms $(g_{(qtz)}\ a)^{-1}$ and fast muonic production rate $P_{\mu fast} = 0.105$ atoms $(g_{(qtz)}\ a)^{-1}$. Production rates are not corrected for snow shielding.

Pinedale and Bull Lake depth profiles (Figures 3b and 4b and Table 1). For the Bull Lake moraine additional grain size fractions are also reported.

[35] In the depth profile of the Pinedale moraine, the ^{10}Be concentrations of the 0.5–1.0 mm grain size fraction range from 1.11 to 3.73 $\times$ 10^5 atoms $g_{(qtz)}^{-1}$ (Table 1 and Figure 3b). The highest nuclide concentrations are measured in the surface samples. The uppermost four samples (3, 10, 20, and 30 cm) show uniform nuclide concentrations of 3.60–3.73 $\times$ 10^5 atoms $g_{(qtz)}^{-1}$. Below this surface layer (>40 cm), the nuclide concentrations decrease with depth. Hence, the lowest nuclide concentration is measured in the deepest sample (133 cm). The nuclide concentrations of the surface samples are roughly three times higher than the concentration of the lowermost sample.

[36] The ^{10}Be concentrations of the 0.5–1 mm grain size fraction range from 4.93 to 14.9 $\times$ 10^5 atoms $g_{(qtz)}^{-1}$ in the depth profile of the Bull Lake moraine (Table 1 and Figure 4b). The uppermost four samples (5, 20, 28, and 43 cm) show a relatively homogenous cosmogenic nuclide concentration ranging from 13.6 to 14.9 $\times$ 10^5 atoms $g_{(qtz)}^{-1}$. However, a slight decrease in the ^{10}Be concentration with depth is observed in this surface layer. Below the surface layer (>50 cm), the nuclide concentrations decrease with depth. The nuclide concentration of the lowermost sample (130 cm) is roughly three times lower than the nuclide concentrations of the surface samples. The cosmogenic nuclide concentrations of smaller grain size fractions (0.125–0.25 mm and 0.25–0.5 mm) in the sample from 104 cm depth indicate only minor grain size dependence. The smaller grain size fraction (0.25–0.5 mm) analyzed for the sample from 43 cm depth has a lower nuclide concentration than the 0.5–1 mm grain size fraction, which might be due to grain size dependence in soil mixing. Cosmogenic nuclide concentrations of samples from the Bull Lake moraine are roughly four to five times higher than nuclide concentrations of samples from the Pinedale moraine at comparable sampling depths.

5.2. Approach A: The Lal and Chen Approach

[37] In the following section the results from the application of the Lal and Chen approach to our data are presented (Figure 5). Predicted and observed ages and denudation rates are plotted as a function of ^{10}Be concentration ratio in the mixed layer and the surface of the stagnant layer versus the concentration in the mixed surface layer. Ages and denudation rates are derived for the measured values on the basis of (1) the nuclide concentration measured in the lowermost sample of the mixed surface layer and the sample just below the mixed surface layer (black squares in Figure 5) and (2) the average nuclide concentration measured in the samples of the mixed surface layer and the sample just below the mixed surface layer (open squares in Figure 5). Ages and denudation rates for the sample just above the mixing zone (case 1) are given below, and the ages and denudation rates based on the

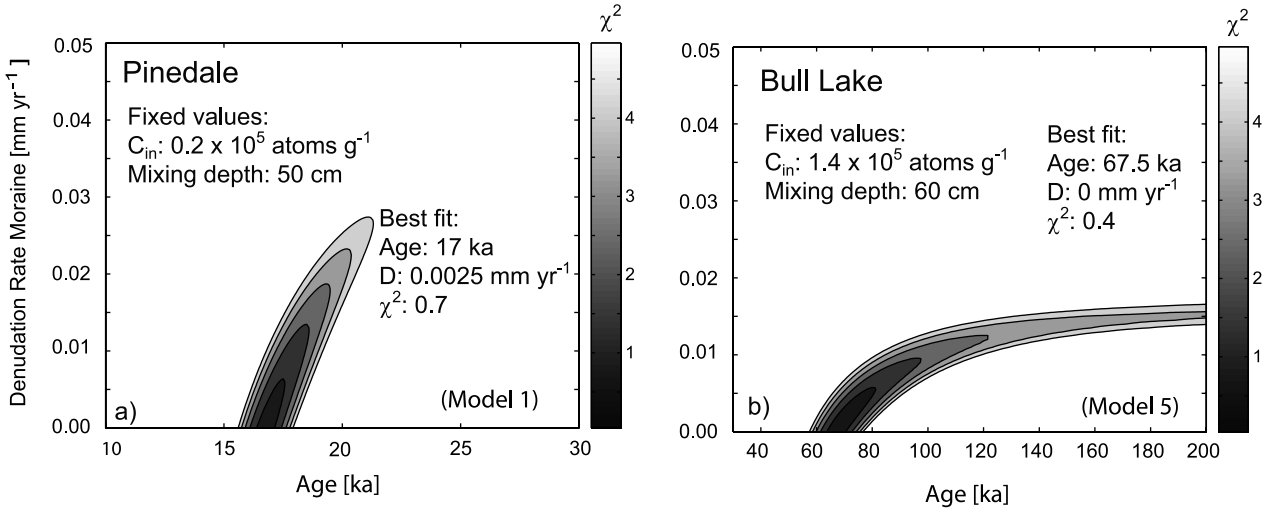

Figure 6. Chi-square analysis for cosmogenic nuclide concentrations of samples from (a) Pinedale moraine and (b) Bull Lake moraine assuming constant denudation rate over time. Constant denudation rate D of the moraine is plotted versus deposition age. The calculations are based on a density of 2.0 g cm^{-3}. The best Chi-square solutions χ^2 are calculated for all samples using a fixed nuclide inheritance (C_{in}) and mixing depth and applying present-day snow shielding.

average nuclide concentrations (case 2) are reported in parenthesis.

[38] The calculated age of the Pinedale moraine based on a mixing depth of 40 cm is ~19 ka (~20 ka) and the denudation rate is ~0.030 mm a^{-1} (~0.035 mm a^{-1}; Figures 5a and 5b). Using deeper mixing depths (e.g., 50 cm) decreases the calculated age to ~17 ka and the denudation rate to ~0.015 mm a^{-1} (not shown). For the Bull Lake moraine, the age based on a mixing depth of 50 cm is ~67 ka (~77 ka) and the denudation rate is ~0.004 mm a^{-1} (~0.007 mm a^{-1}; Figures 5c and 5d). Using a deeper mixing depth (e.g., 60 cm) decreases the calculated age to ~65 ka and the denudation rate to ~0.001 mm a^{-1} (not shown). In summary, ages and denudation rates for the Pinedale moraine range between 17–20 ka and 0.015–0.035 mm a^{-1}, respectively. Ages and denudation rates for the Bull Lake moraine are 65–77 ka and 0.001–0.007 mm a^{-1}, respectively.

5.3. Approach B: Chi-Square Results for Cosmogenic Nuclide Concentrations

[39] In the following section the different Chi-square analyses for constant and transient denudation rates are presented for the Pinedale and Bull Lake moraines (Table 3). The best reduced sum Chi-square solutions assuming present-day snow shielding are calculated for the nuclide concentration measured in the 0.5–1 mm grain size fraction.

5.3.1. Constant Denudation Rate Simulations

[40] The best fit solutions for moraine age and denudation rate for fixed values of the soil mixing depth and inherited nuclide concentration are presented in Figure 6. In the depth profile of the Pinedale moraine, good reduced sum Chi-square solutions (<2) for all samples (using the present-day snow shielding correction) are achieved for ages around 17–18 ka and constant denudation rates of the moraine of 0–0.015 mm a^{-1} (Figure 6a). The lowest reduced sum Chi-square values (0.7–0.9) are achieved with ages of 16.5–17.5 ka, constant denudation rates for the moraine of 0–0.005 mm a^{-1}, a nuclide inheritance of 0.2 × 10^5 atoms g$^{-1}_{(qtz)}$, and complete mixing to a depth of 50 cm (Model 1 in Table 3).

[41] For the depth profile of the Bull Lake moraine good solutions (<2) are achieved for ages of ~60–100 ka and denudation rates of 0–0.010 mm a^{-1} using a production rate correction for present-day snow shielding (Figure 6b). The best Chi-square solutions (0.4–0.5) for all Bull Lake samples are given by ages of 65–72.5 ka, 0–0.003 mm a^{-1} denudation of the moraine, a nuclide inheritance of 1.4–2.0 × 10^5 atoms g$^{-1}_{(qtz)}$, and complete mixing to a depth of 60 cm (Model 5 in Table 3). The constant denudation rates determined in this study are 0.0175 mm a^{-1} for the Pinedale moraine and 0.010 mm a^{-1} for the Bull Lake moraine (Models 2 and 6 in Table 3).

5.3.2. Transient Denudation Rate Simulations

[42] The influence of transient moraine denudation on a Chi-square misfit to the data is shown in Figures 7 and 8. For simplicity, we highlight how two different topographic evolution scenarios provide a similar fit to the present-day topography and observed nuclide concentrations.

[43] A visual comparison between observed topographic profiles and numerical model calculations based on diffusivity, indicate that the good fits for the Pinedale moraine can be achieved with 1) low diffusivity (<1 × 10^{-3} m^2 a^{-1}) with a maximum initial height of 26 m, a slope angle of 20°, and an initial moraine flat-top width of 70 m or 2) high diffusivity (25 × 10^{-3} m^2 a^{-1}) with a maximum height of 27 m, a slope angle of 30°, and a flat width of 100 m (Figures 7a and 7d). These two different assumptions result in very different average denudation rates at the crest position of 0.001 and 0.028 mm a^{-1}, respectively (Figures 7b and 7e). Similar to the constant denudation rate simulations previously presented, the best Chi-square solutions (0.5) for the Pinedale moraine are achieved for ages of 17–24 ka and average denudation rates of 0.003–0.051 mm a^{-1} (Model 3 in Table 3). These average denudation rates correspond to diffusivities of 0.3–30 ×

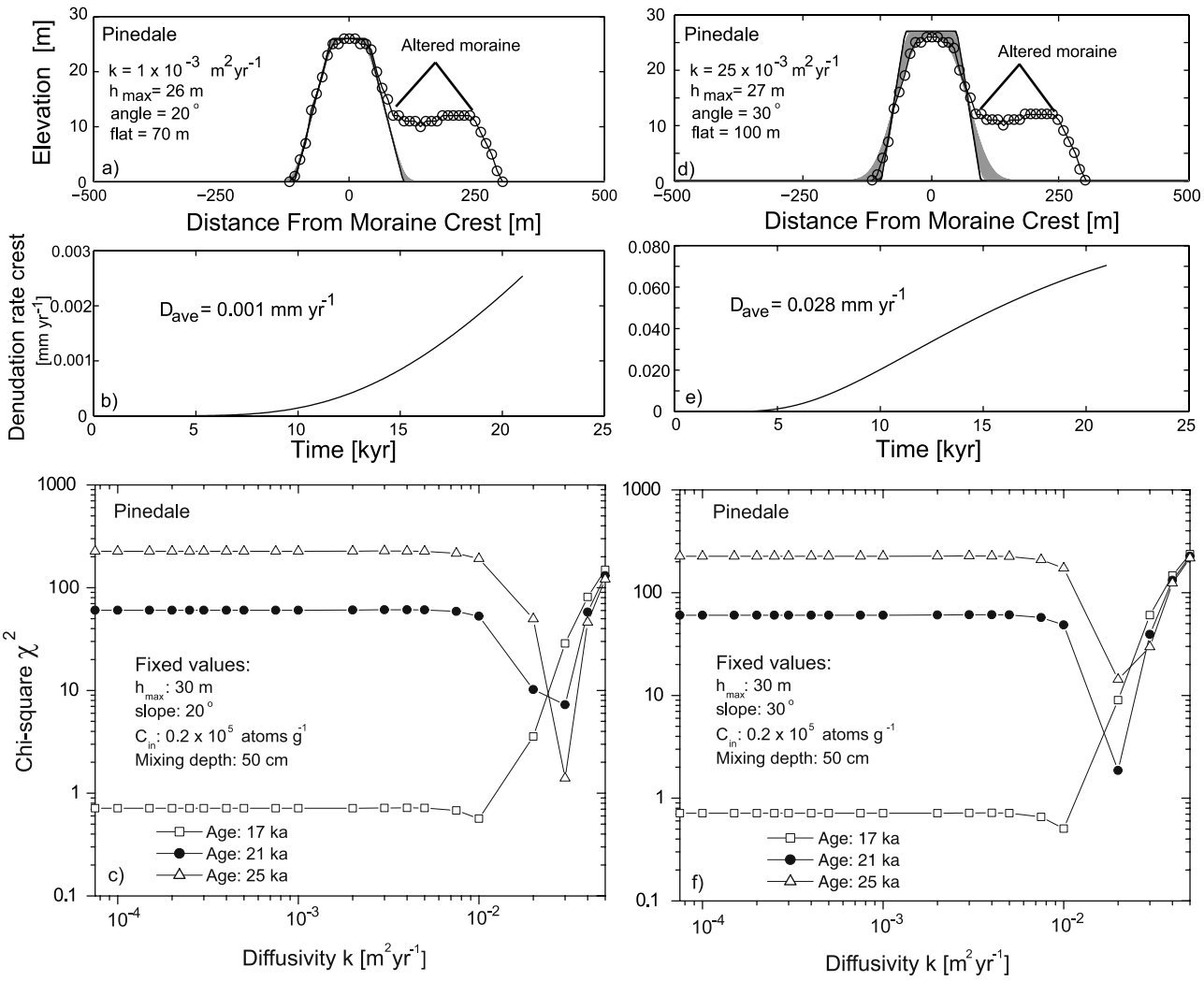

Figure 7. Transient denudation of the Pinedale moraine. (a) The observed topography (open circles) is simulated with a diffusion model (black lines) after *Fernandes and Dietrich* [1997]. A good fit is achieved with low diffusivities (e.g., $k = 1 \times 10^{-3}$ m^2 a^{-1}), a maximum height h_{max} of 26 m, a deposition angle of 20°, and a flat width of 70 m. (b) The denudation rate of the moraine crest over time is calculated with the parameters as determined in Figure 7a. The average denudation rate is 0.001 mm a^{-1}. (c) Chi-square values versus diffusivities for different age constraints. The fixed values are based on the best Chi-square solution for Model 3 in Table 3. (d) Diffusion model as in Figure 7a. A good fit is achieved with high diffusivities (e.g., $k = 25 \times 10^{-3}$ m^2 a^{-1}), a maximum height h_{max} of 27 m, a deposition angle of 30°, and a flat width of 100 m. (e) Transient denudation rate over time as in Figure 7b. (f) Chi-square values over diffusivity as in Figure 7c.

10^{-3} m^2 a^{-1}. The best results are determined for a slope angle of 20°. This slope angle is close to the present-day observed topography of the Pinedale moraine (Figure 7a).

[44] For the Bull Lake moraine, comparison of the observed topographic profile with numerical model calculations based on diffusivity indicate that good fits occur with 1) low diffusivity ($<2 \times 10^{-3}$ m^2 a^{-1}) with a maximum height of 30 m, a slope angle of 5°, and a initial moraine flat-top width of 180 m or 2) high diffusivity (50×10^{-3} m^2 a^{-1}) with a maximum height of 40 m, a slope angle of 30°, and flat width of 250 m (Figures 8a and 8d). These assumptions result in average denudation rates at the crest position of 0 and 0.052 mm a^{-1}, respectively. The best Chi-square solutions (0.4) for the Bull Lake moraine are achieved for ages of 70–127.5 ka and average denudation rates of 0–0.016 mm a^{-1} (Model 7 in Table 3). These best fit solutions are based on diffusivities of $0.1–20 \times 10^{-3}$ m^2 a^{-1}, and slope angles ranging from 5–30°. The best fit solutions for denudation rates based on the samples below the mixed surface and the independent age constraints are 0.032–0.034 mm a^{-1} for the Pinedale moraine (average is 0.033 ± 0.001 mm a^{-1}) and 0.010–0.022 mm a^{-1} for the Bull Lake moraine (average is 0.014 ± 0.004; Models 4 and 8 in Table 3).

6. Discussion

[45] The following sections discuss: (1) the measured cosmogenic nuclide concentrations, (2) Chi-square analysis for constant and transient denudation scenarios, (3) com-

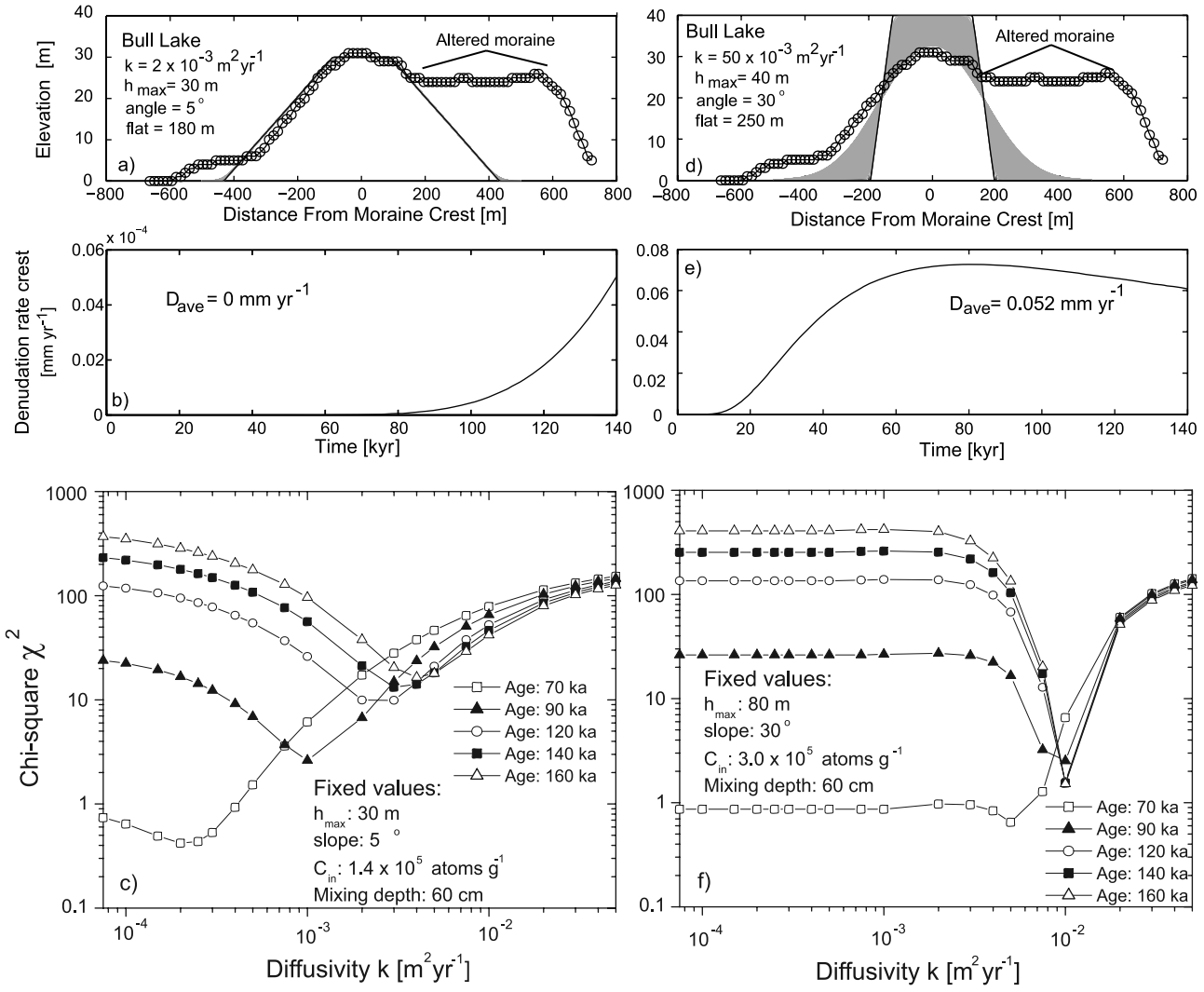

Figure 8. Same as in Figure 7 but for the Bull Lake moraine.

parison of Lal and Chen approach with our Chi-square analysis, and (4) comparison of ages and denudation rates from this study with independent constraints.

6.1. Cosmogenic Nuclide Concentrations

[46] The general pattern in the measured ^{10}Be concentrations of the Pinedale and Bull Lake profiles is similar; a surface layer consisting of relatively uniform nuclide concentrations over continuously decreasing nuclide concentrations (Figures 3b and 4b). The nuclide concentration in the depth profile of the Pinedale moraine shows a uniform nuclide concentration in the surface layer indicative of surface mixing to a depth of ~40 cm (Figure 3b). In contrast, a slight decrease in the nuclide concentration of the samples in the surface layer (~50 cm) is observed in the depth profile of the Bull Lake moraine (Figure 4b). This observation in combination with the differences in nuclide concentrations of different grain sizes may indicate that the Bull Lake surface layer is not completely mixed. Variations in the magnitude of Bull Lake mixing could be because active mixing is only in the uppermost 10–20 cm or the magnitude of mixing is depth dependent. The two depth profiles may therefore show differences in Chi-square analysis due to differences in the degree of mixing.

6.2. Chi-Square Analysis Based on Constant and Transient Denudation Rates

[47] The previous Chi-square analysis of the cosmogenic nuclide concentrations measured in the Pinedale and Bull Lake moraines provided constraints on the depositional age, denudation rate (constant or transient), and the inherited nuclide concentration. In general, a higher nuclide inheritance is calculated for the Bull Lake moraine than for the Pinedale moraine. The high nuclide inheritance might reflect the incorporation of preirradiated reworked till in the Bull Lake moraine. Quartzite cobbles were found in the lower till of the Bull Lake moraines which are described as being derived from older terrace deposits (e.g., the Sacagawea outwash terraces [*Richmond*, 1973]).

[48] The results based on the assumption of transient denudation rates differ only marginally from the results gained from analysis assuming constant denudation rates (Table 3). The inherited nuclide concentration and the mixing depth agree within the resolution of the Chi-square analysis (Models 1 and 3 for the Pinedale moraine and

Models 5 and 7 for the Bull Lake moraine in Table 3). The calculated ages and average denudation rates show a larger range of solutions for the transient denudation rate assumption. For example, the age based on constant denudation rate for the Pinedale moraine is 16.5–17.5 ka whereas the age based on transient denudation rate is 17–24 ka (Model 1 and 3 in Table 3).

[49] The analysis of the observed moraine topographies with the diffusion model indicates multiple solutions for diffusivity, maximum height, slope angle, and flat width, which fit the observed topography equally well (e.g., Figures 7a, 7d, 8a, and 8d). Good solutions for the measured nuclide concentrations are possible with low and high diffusivities. Different geometries of flat-topped, trapezoidal moraines can be used for model calculations to match the measured nuclide concentrations. The sensitivity of the model geometry in the range of small diffusivities is low as it takes time for the moraine crest to evolve at low denudation rates. A flat-topped, trapezoidal moraine seems to be a possible deposition geometry of the terminal end moraines. In the case of the Pinedale moraine, the observed steeper slope angles compared to the Bull Lake moraine, could be the result of the younger age as well as the existence of the Bull Lake moraine in front of the Pinedale moraine. Unfortunately we have no way of independently constraining the moraine geometries at the time of deposition and additional analysis based on different depositional geometries would be poorly constrained.

6.3. Comparison of Lal and Chen Approach With Chi-Square Analysis

[50] In this section we address whether the Lal and Chen approach (Approach A) results in fundamentally different solutions than the Chi-square analysis for constant and transient moraine denudation (Approach B). In general, the results agree well for the Bull Lake moraine and the Pinedale moraine. In the case of the Bull Lake moraine, the age (~67 ka) and denudation rate (~0.004 mm a^{-1}) determined with the Lal and Chen approach using a mixing depth of 50 cm (Figures 5c and 5d) are comparable to the results from the Chi-square analysis (70–127.5 ka and 0–0.016 mm a^{-1}; Table 3). The primary advantage of the Chi-square approach is that the range of possible parameters that can fit the observed nuclide concentrations can be identified, rather than single values.

[51] In the case of the Pinedale moraine, the age (~19 ka) and denudation rate (~0.030 mm a^{-1}) based on the Lal and Chen approach and using a mixing depth of 40 cm (Figures 5a and 5b) compare with ages (17–24 ka) and denudation rates (0–0.051 mm a^{-1}) determined with the Chi-square analysis (Table 3). Using deeper mixing depth in the Lal and Chen approach results in lower ages and denudation rates fitting well with the lower values derived from the Chi-square approach. The choice of the mixing depth that is used is an important factor in the Lal and Chen approach such that a detailed and careful investigation of the depth profile is required not only to determine the mixing depth, but also for selecting the samples used for cosmogenic nuclide analysis and subsequent calculations. An additional disadvantage of the Lal and Chen approach is that it does not take into account nuclide inheritance. Differences between the Lal and Chen approach and the Chi-square analysis might also result from different sensitivities of the two methods to the selected density as well as the applied snow correction.

[52] In summary, we find that the approach of Lal and Chen matches well with the more sophisticated numerical approach. Whereas the Chi-square approach requires several samples from different depths (~2 m), the Lal and Chen approach is based on only two samples from the upper part of the depth profile (~60 cm). However, the age and denudation rate determination based on only two samples requires a careful evaluation of the mixing depth and the sample selection. Evaluation of the mixing depth in the field may not always be possible. We conclude that the Lal and Chen approach is best applied in settings where the mixing depth is well constrained from other methods, sample selection is straightforward, mixing is complete, and nuclide inheritance is assumed to be minimal. In practice, the previous restrictions will likely prohibit widespread application of this approach.

6.4. Comparison of Ages and Denudation Rates With Independent Constraints

6.4.1. Age Comparison

[53] In the following section we compare ages determined from cosmogenic nuclides in depth profiles with independent age constraints from the literature. The best estimated independent ages are considered to be ~21 ka for the Pinedale moraine and ~140 ka for the Bull Lake moraine (see section 2.2).

[54] Moraine ages determined with cosmogenic nuclides measured in depth profiles are generally younger than the previous independent age constraints for the Pinedale and Bull Lake moraines, respectively. In the following we demonstrate how the mixing degree and depth could influence our age determinations from depth profiles.

[55] To demonstrate the influence of complete mixing of variable depths on moraine age we analyzed each depth profile with the Chi-square model using only age and mixing depth as free parameters (Figures 9a and 9b). The inherited nuclide concentration C_{in}, the diffusivity k, the maximum height h_{max}, and the slope angle are fixed to the values as determined in the best Chi-square solution for the transient denudation model (Models 3 and 7 for Pinedale and Bull Lake moraines in Table 3). In the case of the Pinedale moraine, Chi-square solutions $\chi^2 < 2$ are achieved for mixing depths between ~40 and ~50 cm (Figure 9a). This is in good agreement with the observed mixing depth from the cosmogenic nuclide concentrations (Figure 3b). The comparable analysis for the Bull Lake moraine (fixed values from Model 7 in Table 3) results also in a best Chi-square solution ($\chi^2 < 2$) for mixing depths between ~30 and ~60 cm (Figure 9b). In the case of the Bull Lake moraine, possible solutions are not only restricted to the depth determined from the measured nuclide concentrations, but range also from 0 to 30 cm. This result may indicate that the surface layer of the Bull Lake moraine is incompletely mixed (e.g., different mixing depth and depth-dependent mixing).

[56] We also analyzed the effect of incomplete mixing on the age calculation (Figures 10a and 10b). The best solution for the transient denudation rate model based on samples below the mixed surface layer and the independent age

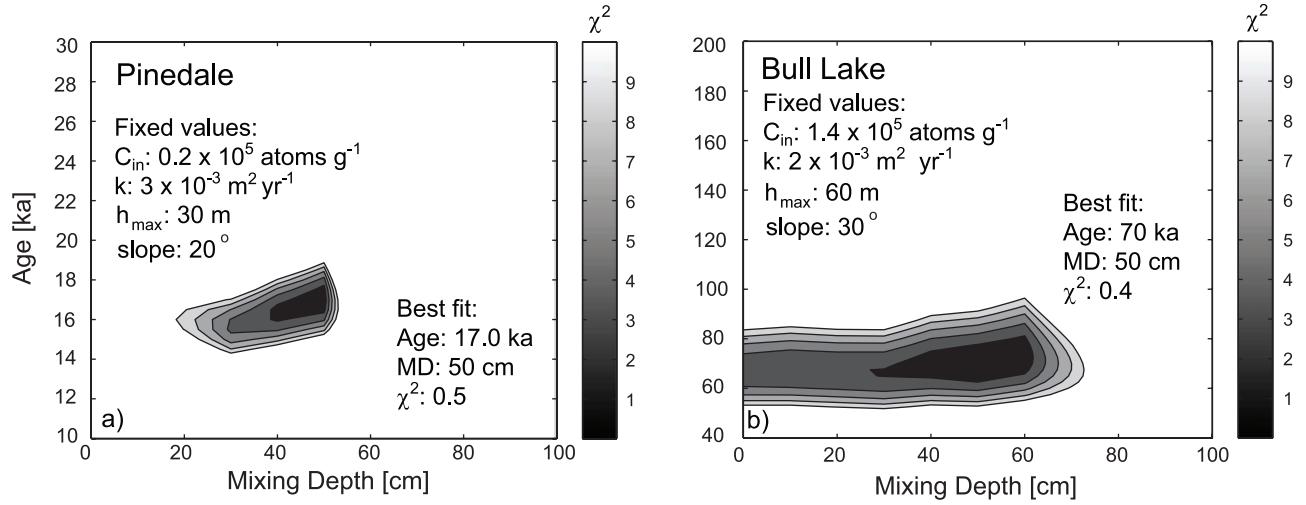

Figure 9. Age versus mixing depth is shown for the (a) Pinedale moraine and (b) Bull Lake moraine assuming transient denudation rate and taking into account correction for present-day snow shielding. The results for the Pinedale moraine indicate a single best solution at a mixing depth of 50 cm. The results for the Bull Lake moraine show a wide range for the mixing.

constraint (Models 4 and 8 in Table 3) are used to calculate the nuclide concentration in samples. The assumption of no mixing and mixing to a given depth is made (50 and 60 cm for the Pinedale and Bull Lake moraines, respectively). In the case of complete mixing, we expect that the measured and calculated nuclide concentrations agree. This approach is valid under the additional assumption that using the samples from below the mixed surface layer and the independent age to constrain the fixed values is justified. For the Bull Lake moraine, the calculated nuclide concentrations in the mixed surface layer are higher than the measured nuclide concentrations (Figure 10) whereas for the Pinedale moraine the calculated nuclide concentrations in the mixed surface layer are comparable to the measured nuclide concentrations. This might indicate that the surface layer is mixed in the Bull Lake moraine, but not to completion as suggested by the model assumption (e.g., different lines shown in Figure 2b).

[57] Because of this lower than expected nuclide concentration in the surface layer of the Bull Lake moraine, ages based on the assumption of complete mixing are younger than the independent ages (up to 70 ka). These younger ages are predicted because the model assumes complete mixing, however the Bull Lake moraine is only partially mixed. From the model simulation based on no mixing of the surface layer it appears that the measured nuclide concen-

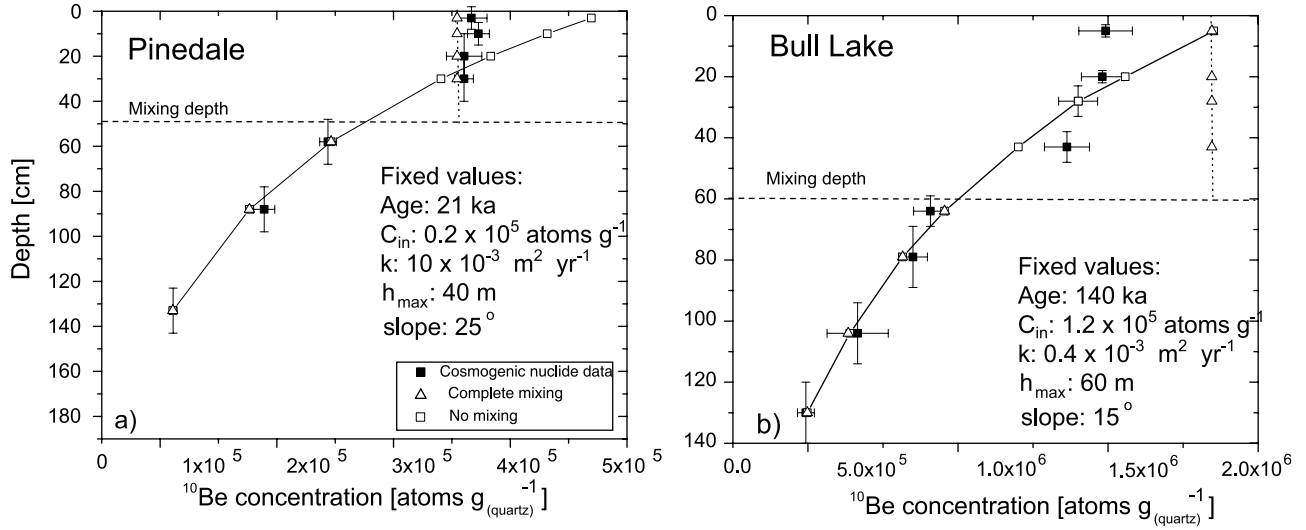

Figure 10. Depth in soil pit versus nuclide concentration for the (a) Pinedale moraine and (b) Bull Lake moraine. The measured nuclide concentrations (solid squares) are compared to modeled nuclide concentrations based on results from samples below the surface layer. The nuclide concentrations in the surface layer are modeled assuming (1) complete mixing to a given depth (open triangles) and (2) no mixing (open squares). Mixing depths for model simulations are assumed to be 50 cm for the Pinedale moraine and 60 cm for the Bull Lake moraine.

trations in the Bull Lake moraine are close to the average concentration of the unmixed surface layer to a given depth. This can be attained if the mixing in the surface layer occurred recently. We conclude that the nuclide concentration in the surface layer has been homogenized, but mixing is not complete in the case of the Bull Lake moraine. The degree of mixing is difficult to constrain (e.g., because of restricted data resolution, uncertainty in production rate and density etc.). Thus, we find that the assumption of complete mixing in a homogenized surface layer [e.g., *Lal and Chen*, 2005, 2006] needs to be evaluated before calculating ages and denudation rates. Results based on the assumption of complete mixing where the surface layer is not completely mixed may be erroneous.

[58] In summary, age constraints from depth profiles of coarse material in areas where climatic conditions require snow shielding corrections and where mixing in the surface layer is not thorough are difficult to interpret. Ages from exposure age dating of boulders are more straightforward than ages from depth profiles. Although boulder exposure ages are influenced by uncertainties related to snow shielding and/or exhumation due to denudation of surrounding soil, this is generally a smaller uncertainty for boulder age determination than for the depth profile technique.

6.4.2. Denudation Rate Comparison

[59] Denudation rates calculated with the Chi-square approach and data from all samples in a profile are most likely also affected by unknown degrees of mixing. Therefore, we consider the denudation rates based on the samples below the mixed layer and the independent age constraint to be more reliable than denudation rates based on all samples. The constant denudation rates determined in this study are 0.0175 mm a^{-1} for the Pinedale moraine and 0.010 mm a^{-1} for the Bull Lake moraine. Slightly higher rates are calculated for the transient denudation rate of 0.032–0.034 mm a^{-1} for the Pinedale moraine (average is 0.033 ± 0.001 mm a^{-1}) and 0.010–0.022 mm a^{-1} for the Bull Lake moraine (average is 0.014 ± 0.004 mm a^{-1}). The average denudation rates from the constant and transient cases are 0.025 mm a^{-1} for the Pinedale moraine and 0.012 mm a^{-1} for the Bull Lake moraine. These denudation rates and the associated independent age constraints result in net denudation of 0.525 and 1.68 m for the Pinedale and Bull Lake moraines, respectively. The results from terminal moraines in the Wind River Mountains (0.012 and 0.025 mm a^{-1}) are in agreement with denudation rate determinations based on boulder age considerations and boulder heights in the western Wind River Mountains (0.010 mm a^{-1}; see section 2.3). The denudation rates from this study agree with other rates derived from exhumation modeling of boulder surfaces and depth profile dating (0.005–0.060 mm a^{-1}). However, denudation rates derived from diffusion models of surface degradation of lateral moraines (0.28–0.7 mm a^{-1}) are generally an order of magnitude higher than denudation rates determined in this study for terminal end moraines.

7. Summary and Conclusions

[60] The cosmogenic nuclide concentrations measured in two shallow depth profiles (~1.5 m) from the Pinedale (independent age constraint is ~21 ka) and Bull Lake (independent age constraint is ~140 ka) moraines in the Fremont Lake area (Wyoming, United States) reveal the following:

[61] 1. In situ–produced cosmogenic nuclide concentrations measured in the surface layer of the two moraine deposits are relatively homogenous. The surface layer of the Pinedale moraine seems to be mixed to a depth of 40–50 cm whereas the surface layer of the Bull Lake moraine seems to be mixed to a depth of 50–60 cm.

[62] 2. Chi-square analyses of predicted and observed nuclide concentration from the two depth profiles were conducted to explore the effect of constant and transient denudation on nuclide concentrations. In the case of low denudation rates as determined from the nuclide concentrations measured in this study, there is no significant difference in the calculated ages and denudation rates using the constant or transient denudation approach. Ages calculated assuming present-day snow shielding are 16.5–24 ka and 65–127.5 ka for the Pinedale moraine and Bull Lake moraine, respectively. These ages are comparable or younger than independent age constraints derived from the literature due to the influence of incomplete surface mixing on cosmogenic depth profile dating.

[63] 3. Diffusion models of moraine topographic evolution were conducted for flat-topped, trapezoidal moraine geometry ranging in hillslope depositional angles, moraine crest heights, and flat-top width. A wide range of simulated diffusivities and moraine geometries can fit the observed cosmogenic nuclide concentrations.

[64] 4. Uncertainties in moraine denudation rate estimates can be caused by soil mixing. To avoid this, we suggest using samples below the mixed surface layer in combination with independent age constraints to improve denudation rate estimates. For the Fremont Lake moraines, average denudation rates based on constant denudation rates, present-day snow shielding, and independent age constraints are 0.0175 mm a^{-1} for the Pinedale moraine and 0.010 mm a^{-1} for the Bull Lake moraine. Results from our transient denudation simulations suggest average denudation rates are 0.032 mm a^{-1} for the Pinedale moraine and 0.014 mm a^{-1} for the Bull Lake moraine. Net denudation of the Pinedale and Bull Lake moraines are estimated to be 0.525 and 1.68 m, respectively.

[65] 5. Ages and denudation rates derived from the Lal and Chen approach agree relatively well with results from the Chi-square analysis, although a wider range of permissionable solutions is identified through the Chi-square analysis. As the Lal and Chen approach is sensitive to the selected mixing depth and relies on two samples from within and below the mixed surface layer, the mixing zone needs to be carefully determined in the field.

[66] 6. The technique of depth profile dating for age and denudation rate determination in shallow depth profiles is sensitive to soil mixing, snow shielding correction and density. Age and denudation rates are difficult to constrain on flat terminal moraines. Boulder exposure ages seem to be more reliable for moraine age determination. However, depth profiles are effective at determining mixing depth and determining denudation rates.

[67] 7. The nuclide concentrations measured in the surface layers of the Pinedale and Bull Lake moraines are homogenized to a depth of ~50 and ~60 cm, respectively.

Model calculations seem to indicate that the surface layers are mixed, but in the case of the Bull Lake moraine not completely mixed (e.g., recent mixing, different mixing depths and depth-dependent mixing degree).

[68] 8. The denudation rates determined for the Pinedale and Bull Lake moraine crests are in good agreement with other studies based on cosmogenic nuclides. However, denudation rates used in diffusion models of surface degradation of lateral moraines are generally 1 order of magnitude higher than denudation rates determined in this study on terminal moraines.

[69] 9. Contrary to assumptions of previous chemical weathering studies we find that moraine crests in the Fremont Lake area do erode significantly and that soils are significantly mixed. Weathering rates and dust accumulation rates calculated on the assumption of no denudation and no mixing of the surface layer are underestimated and need to be reevaluated.

[70] **Acknowledgments.** We would like to thank Matt Densmore for assistance in the field. The constructive reviews of F. Phillips, G. Hilley, J. Putkonen, G. Balco, and an anonymous reviewer considerably improved the manuscript. This study was supported through a seed fund of PRIME Lab, a Swiss Science Foundation postdoctoral fellowship to M.S., and a National Science Foundation grant to T.A.E. (EAR-0544954).

References

Anderson, R. S., J. L. Repka, and G. S. Dick (1996), Explicit treatment of inheritance in dating depositional surfaces using in situ ^{10}Be and ^{26}Al, *Geology*, *24*(1), 47–51, doi:10.1130/0091-7613(1996)024<0047:ETOIID>2.3.CO;2.

Barnosky, C., P. Anderson, and P. Bartlein (1987), The northwestern U.S. during deglaciation: Vegetational history and paleoclimatic implications, in *North America and Adjacent Oceans During the Last Deglaciation*, edited by W. F. Ruddiman and H. E. Wright, pp. 289–323, Geol. Soc. of Am., Boulder, Colo.

Benson, L., R. Madole, W. M. Phillips, G. P. Landis, T. Thomas, and P. W. Kubik (2004), The probable importance of snow and sediment shielding on cosmogenic ages of north-central Colorado Pinedale and pre-Pinedale moraines, *Quat. Sci. Rev.*, *23*(1–2), 193–206, doi:10.1016/j.quascirev.2003.07.002.

Benson, L., R. Madole, G. Landis, and J. Gosse (2005), New data for late Pleistocene Pinedale alpine glaciation from southwestern Colorado, *Quat. Sci. Rev.*, *24*, 49–65, doi:10.1016/j.quascirev.2004.07.018.

Braucher, R., P. Del Castillo, L. Siame, A. J. Hidy, and D. L. Bourlés (2008), Determination of both exposure time and denudation rate from an in situ-produced ^{10}Be depth profile: A mathematical proof of uniqueness. Model sensitivity and applications to natural cases, *Quat. Geochronol.*, *4*, 56–67.

Brown, E. T., D. L. Bourlés, F. Colin, G. M. Raisbeck, F. Yiou, and S. Desgarceaux (1995), Evidence for muon-induced production of ^{10}Be in near-surface rocks from the Congo, *Geophys. Res. Lett.*, *22*(6), 703–706, doi:10.1029/95GL00167.

Brown, E. T., D. L. Bourles, B. C. Burchfiel, D. Qidong, L. Jun, P. Molnar, G. M. Raisbeck, and F. Yiou (1998), Estimation of slip rates in the southern Tien Shan using cosmic ray exposure dates of abandoned alluvial fans, *Geol. Soc. Am. Bull.*, *110*(3), 377–386, doi:10.1130/0016-7606(1998)110<0377:EOSRIT>2.3.CO;2.

Dahms, D. E. (2002), Glacial stratigraphy of Stough Creek Basin, Wind River Range, Wyoming, *Geomorphology*, *42*, 59–83, doi:10.1016/S0169-555X(01)00073-3.

Day, P. R. (1965), Particle fractionation and particle-size analysis, in *Methods of Soil Analysis, Part 1*, edited by C. A. Black, pp. 545–567, Am. Soc. of Agronomy, Madison, Wis.

Dunai, T. J. (2000), Scaling factors for production rates of in situ produced cosmogenic nuclides: A critical reevaluation, *Earth Planet. Sci. Lett.*, *176*(1), 157–169, doi:10.1016/S0012-821X(99)00310-6.

Easterbrook, D. J., K. Pierce, J. Gosse, A. Gillespie, E. Evenson, and K. Hamblin (2003), Quaternary geology of the western United States, in *Quaternary Geology of the United States*, edited by D. J. Easterbrook, pp. 19–79, Desert Res. Inst., Reno, Nev.

Ehlers, T. A., S. D. Willett, P. A. Armstrong, and D. S. Chapmanm (2003), Exhumation of the central Wasatch Mountains, Utah: 2. Thermokinematic model of exhumation, erosion, and themochronometer interpretation, *J. Geophys. Res.*, *108*(B3), 2173, doi:10.1029/2001JB001723.

Fernandes, N. F., and W. E. Dietrich (1997), Hillslope evolution by diffusive processes: The timescale for equilibrium adjustments, *Water Resour. Res.*, *33*(6), 1307–1318, doi:10.1029/97WR00534.

Gosse, J. C., and F. M. Phillips (2001), Terrestrial in situ cosmogenic nuclides: Theory and application, *Quat. Sci. Rev.*, *20*, 1475–1560, doi:10.1016/S0277-3791(00)00171-2.

Gosse, J. C., J. Klein, E. B. Evenson, B. Lawn, and R. Middleton (1995), Beryllium-10 dating of the duration and retreat of the last Pinedale glacial sequence, *Science*, *268*, 1329–1333, doi:10.1126/science.268.5215.1329.

Granger, D. E., and A. L. Smith (2000), Dating buried sediments using radioactive decay and muogenic production of ^{26}Al and ^{10}Be, *Nucl. Instrum. Methods Phys. Res. Sect. B*, *172*, 822–826, doi:10.1016/S0168-583X(00)00087-2.

Hall, R. D., and R. R. Shroba (1993), Soils developed in the glacial deposits of the type areas of the Pinedale and Bull Lake glaciations, Wind River Range, Wyoming, U.S.A., *Arct. Alp. Res.*, *25*(4), 368–373, doi:10.2307/1551919.

Hall, R. D., and R. R. Shroba (1995), Soil evidence for a glaciation intermediate between the Bull Lake and Pinedale glaciations at Fremont Lake, Wind River Range, Wyoming, U.S.A., *Arct. Alp. Res.*, *27*(1), 89–98, doi:10.2307/1552071.

Hallet, B., and J. Putkonen (1994), Surface dating of dynamic landforms: Young boulders on aging moraines, *Science*, *265*(5174), 937–940, doi:10.1126/science.265.5174.937.

Hancock, G. S., R. S. Anderson, O. A. Chadwick, and R. C. Finkel (1999), Dating fluvial terraces with ^{10}Be and ^{26}Al profiles: Application to the Wind River, Wyoming, *Geomorphology*, *27*(1–2), 41–60, doi:10.1016/S0169-555X(98)00089-0.

Heisinger, B., D. Lal, A. J. T. Jull, P. W. Kubik, S. Ivy-Ochs, S. Neumaier, K. Knie, V. Lazarev, and E. Nolte (2002a), Production of selected cosmogenic radionuclides by muons: Part 1. Fast muons, *Earth Planet. Sci. Lett.*, *200*(3–4), 345–355, doi:10.1016/S0012-821X(02)00640-4.

Heisinger, B., D. Lal, A. J. T. Jull, P. W. Kubik, S. Ivy-Ochs, K. Knie, and E. Nolte (2002b), Production of selected cosmogenic radionuclides by muons: Part 2. Capture of negative muons, *Earth Planet. Sci. Lett.*, *200*(3–4), 357–369, doi:10.1016/S0012-821X(02)00641-6.

Hetzel, R., S. Niedermann, S. Ivy-Ochs, P. Kubik, M. Tao, and B. Gao (2002), ^{12}Ne versus ^{10}Be and ^{26}Al exposure ages of fluvial terraces: The influence of crustal Ne in quartz, *Earth Planet. Sci. Lett.*, *201*(3–4), 575–591, doi:10.1016/S0012-821X(02)00748-3.

Lal, D., and J. Chen (2005), Cosmic ray labeling of erosion surfaces II: Special cases of exposure histories of boulders, soils and beach terraces, *Earth Planet. Sci. Lett.*, *236*, 797–813, doi:10.1016/j.epsl.2005.05.025.

Lal, D., and J. Chen (2006), Erratum to "Cosmic ray labeling of erosion surfaces II: Special cases of exposure histories of boulders, soils and beach terraces", *Earth Planet. Sci. Lett.*, *241*, 360, doi:10.1016/j.epsl.2005.11.002.

Licciardi, J. M., and K. L. Pierce (2008), Cosmogenic exposure-age chronologies of Pinedale and Bull Lake glaciations in greater Yellowstone and the Teton Range, USA, *Quat. Sci. Rev.*, *27*, 814–831, doi:10.1016/j.quascirev.2007.12.005.

Masarik, J., M. Frank, J. M. Schäfer, and R. Wieler (2001), Correction of in situ cosmogenic nuclide production rates for geomagnetic field intensity variations during the past 800,000 years, *Geochim. Cosmochim. Acta*, *65*(17), 2995–3003, doi:10.1016/S0016-7037(01)00652-4.

Meierding, T. C. (1984), Correlation of Rocky Mountain Pleistocene deposits by relative dating methods: A perspective, in *Correlation of Quaternary Chronologies*, edited by W. C. Manahey, pp. 455–477, Geo Books, Norwich, UK.

Perg, L. A., R. S. Anderson, and R. C. Finkel (2001), Use of a new ^{10}Be and ^{26}Al inventory method to date marine terraces, Santa Cruz, California, USA, *Geology*, *29*(10), 879–882, doi:10.1130/0091-7613(2001)029<0879:UOANBA>2.0.CO;2.

Phillips, F. M., M. G. Zreda, J. C. Gosse, J. Klein, E. B. Evenson, R. D. Hall, O. A. Chadwick, and P. Sharma (1997), Cosmogenic ^{36}Cl and ^{10}Be ages of Quaternary glacial and fluvial deposits of the Wind River Range, Wyoming, *Geol. Soc. Am. Bull.*, *109*(11), 1453–1463, doi:10.1130/0016-7606(1997)109<1453:CCABAO>2.3.CO;2.

Phillips, F. M., M. G. Zreda, T. M. Shanahan, M. I. Bursik, and M. A. Plummer (2000), Cosmogenic depth profiles and erosion modeling: New results for the Bloody Canyon moraines, Mono Basin, California, *Eos Trans. AGU*, *81*(48), Fall Meet. Suppl., Abstract U22B-10.

Phillips, F. M., M. G. Zreda, M. A. Plummer, D. Elmore, and D. H. Clark (2008), Glacial geology and chronology of Bishop Creek and vicinity, eastern Sierra Nevada, California, *Geol. Soc. Am. Bull.*, in press.

Putkonen, J., and M. O'Neal (2006), Degradation of unconsolidated Quaternary landforms in the western North America, *Geomorphology*, *75*(3–4), 408–419, doi:10.1016/j.geomorph.2005.07.024.

Putkonen, J., and T. Swanson (2003), Accuracy of cosmogenic ages for moraines, *Quat. Res.*, *59*, 255–261, doi:10.1016/S0033-5894(03)00006-1.

Putkonen, J., J. Connolly, and T. Orloff (2008), Landscape evolution degrades the geologic signature of past glaciation, *Geomorphology*, *97*(1–2), 208–217, doi:10.1016/j.geomorph.2007.02.043.

Repka, J., R. Anderson, and R. Finkel (1997), Cosmogenic dating of fluvial terraces, Fremont River, Utah, *Earth Planet. Sci. Lett.*, *152*(1–4), 59–73, doi:10.1016/S0012-821X(97)00149-0.

Richmond, G. M. (1973), Geological map of the Fremont Lake South quadrangle, Sublette County, Wyoming, *Geol. Quadrangle Map GQ-458*, U.S. Geol. Surv., Reston, Va.

Richmond, G. M. (1987), Type Pinedale Till in the Fremont Lake area, Wind River Range, Wyoming, in *Centennial Field Guide Volume 2: Rocky Mountain Section of the Geological Society of America*, edited by S. S. Beus, vol. 2, pp. 201–204, Geol. Soc. of Am., Boulder, Colo.

Roering, J. J., J. W. Kirchner, and W. E. Dietrich (2001), Hillslope evolution by nonlinear, slope-dependent transport: Steady state morphology and equilibrium adjustment timescales, *J. Geophys. Res.*, *106*(B6), 16,499–16,513.

Schaller, M., and T. A. Ehlers (2006), Limits to quantifying climate driven changes in denudation rates with cosmogenic radionuclides, *Earth Planet. Sci. Lett.*, *248*, 138–152, doi:10.1016/j.epsl.2006.05.027.

Schaller, M., F. von Blanckenburg, N. Hovius, and P. W. Kubik (2001), Large-scale erosion rates from in situ-produced cosmogenic nuclides in European river sediments, *Earth Planet. Sci. Lett.*, *188*, 441–458, doi:10.1016/S0012-821X(01)00320-X.

Schaller, M., F. von Blanckenburg, A. Veldkamp, L. A. Tebbens, N. Hovius, and P. W. Kubik (2002), A 30,000 yr record of erosion rates from cosmogenic ^{10}Be in Middle European river terraces, *Earth Planet. Sci. Lett.*, *204*(1–2), 307–320, doi:10.1016/S0012-821X(02)00951-2.

Schildgen, T. F., W. M. Phillips, and R. S. Purves (2005), Simulation of snow shielding corrections for cosmogenic nuclide surface exposure studies, *Geomorphology*, *64*, 67–85, doi:10.1016/j.geomorph.2004.05.003.

Shanahan, T., and M. Zreda (2000a), New constraints on the ages of old moraines: The impact of erosion on surface exposure age distributions, *EOS Trans. AGU*, *81*(48), Fall Meet. Suppl., Abstract U21A-12.

Shanahan, T., and M. Zreda (2000b), Chronology of Quaternary glaciations in east Africa, *Earth Planet. Sci. Lett.*, *177*(1–2), 23–42, doi:10.1016/S0012-821X(00)00029-7.

Sharp, W. D., K. R. Ludwig, O. A. Chadwick, R. Amundson, and L. L. Glaser (2003), Dating fluvial terraces by 230Th/U on pedogenic carbonate, Wind River Basin, Wyoming, *Quat. Res.*, *59*, 139–150, doi:10.1016/S0033-5894(03)00003-6.

Siame, L. L., et al. (2004), Local erosion rates versus active tectonics: Cosmic ray exposure modelling in Provence (south-east France), *Earth Planet. Sci. Lett.*, *220*, 345–364, doi:10.1016/S0012-821X(04)00061-5.

Stone, J. O. (2000), Air pressure and cosmogenic isotope production, *J. Geophys. Res.*, *105*(B10), 23,753–23,759.

Taylor, A., and J. D. Blum (1995), Relation between soil age and silicate weathering rates determined from the chemical evolution of a glacial chronosequence, *Geology*, *23*(11), 979–982, doi:10.1130/0091-7613(1995)023<0979:RBSAAS>2.3.CO;2.

Trull, T. W., E. T. Brown, B. Marty, G. M. Raisbeck, and F. Yiou (1995), Cosmogenic ^{10}Be and ^{3}He accumulation in Pleistocene beach terraces in Death Valley, California, U.S.A.: Implications for cosmic-ray exposure dating of young surfaces in hot climates, *Chem. Geol.*, *119*, 191–207, doi:10.1016/0009-2541(94)00092-M.

von Blanckenburg, F., N. S. Belshaw, and R. K. O'Nions (1996), Separation of ^{9}Be and cosmogenic ^{10}Be from environmental material and SIMS isotope dilution analysis, *Chem. Geol.*, *129*, 93–99, doi:10.1016/0009-2541(95)00157-3.

Weather Bureau (1965), Climatic summary of the United States: Supplement for 1951–1960, *Climatogr. Rep. 86-42*, U.S. Gov. Print. Off., Washington, D. C.

Whipp, D. M., T. A. Ehlers, A. E. Blythe, K. W. Huntington, K. V. Hodges, and D. W. Burbank (2007), Plio-Quaternary erosion and kinematic history of the central Nepalese Himalaya: 2. Thermokinematic model of thermochronometer exhumation, *Tectonics*, *26*, TC3003, doi:10.1029/2006TC001991.

Wolkowinsky, A. J., and D. E. Granger (2004), Early Pleistocene incision of the San Juan River, Utah, dated with ^{26}Al and ^{10}Be, *Geology*, *32*(9), 749–752, doi:10.1130/G20541.1.

Zimmerman, S. G., E. B. Evenson, and J. C. Gosse (1994), Extensive boulder erosion resulting from a range fire on the type-Pinedale moraines, Fremont Lake, Wyoming, *Quat. Res.*, *42*, 255–265, doi:10.1006/qres.1994.1076.

Zreda, M. G., and F. M. Phillips (1995), Insights into alpine moraine development from cosmogenic ^{36}Cl buildup dating, *Geomorphology*, *14*, 149–156, doi:10.1016/0169-555X(95)00055-9.

Zreda, M. G., F. M. Phillips, and D. Elmore (1994), Cosmogenic 36Cl accumulation in unstable landforms: 2. Simulation and measurements on eroding moraines, *Water Resour. Res.*, *30*(11), 3127–3136, doi:10.1029/94WR00760.

J. D. Blum, T. A. Ehlers, and M. Schaller, Department of Geological Sciences, University of Michigan, 2534 C. C. Little Building, 1100 North University Avenue, Ann Arbor, MI 48109-1005, USA. (mirjam@umich.edu)

M. A. Kallenberg, International School of Stavanger, Treskeveien 3, N-4043 Hafrsfjord, Norway.